Molecular Biology of the Cell
Vol. 12, 863–879, April 2001

Urokinase Receptor and Fibronectin Regulate the ERK^{MAPK} to p38^{MAPK} Activity Ratios That Determine Carcinoma Cell Proliferation or Dormancy In Vivo

Julio A. Aguirre-Ghiso, David Liu, Andrea Mignatti, Katherine Kovalski, and Liliana Ossowski*

Rochelle Belfer Chemotherapy Foundation Laboratory, Division of Medical Oncology, Department of Medicine, Mount Sinai School of Medicine, New York, New York 10029

Submitted August 28, 2000; Revised November 29, 2000; Accepted January 30, 2001
Monitoring Editor: Tony Hunter

We discovered that a shift between the state of tumorigenicity and dormancy in human carcinoma (HEp3) is attained through regulation of the balance between two classical mitogen-activated protein kinase (MAPK)-signaling pathways, the mitogenic extracellular regulated kinase (ERK) and the apoptotic/growth suppressive stress-activated protein kinase 2 (p38^{MAPK}), and that urokinase plasminogen activator receptor (uPAR) is an important regulator of these events. This is a novel function for uPAR whereby, when expressed at high level, it enters into frequent, activating interactions with the $\alpha5\beta1$-integrin, which facilitates the formation of insoluble fibronectin (FN) fibrils. Activation of $\alpha5\beta1$-integrin by uPAR generates persistently high level of active ERK necessary for tumor growth in vivo. Our results show that ERK activation is generated through a convergence of two pathways: a positive signal through uPAR-activated $\alpha5\beta1$, which activates ERK, and a signal generated by the presence of FN fibrils that suppresses p38 activity. When fibrils are removed or their assembly is blocked, p38 activity increases. Low uPAR derivatives of HEp3 cells, which are growth arrested (dormant) in vivo, have a high p38/ERK activity ratio, but in spite of a similar level of $\alpha5\beta1$-integrin, they do not assemble FN fibrils. However, when p38 activity is inhibited by pharmacological (SB203580) or genetic (dominant negative-p38) approaches, their ERK becomes activated, uPAR is overexpressed, $\alpha5\beta1$-integrins are activated, and dormancy is interrupted. Restoration of these properties in dormant cells can be mimicked by a direct re-expression of uPAR through transfection with a uPAR-coding plasmid. We conclude that overexpression of uPAR and its interaction with the integrin are responsible for generating two feedback loops; one increases the ERK activity that feeds back by increasing the expression of uPAR. The second loop, through the presence of FN fibrils, suppresses p38 activity, further increasing ERK activity. Together these results indicate that uPAR and its interaction with the integrin should be considered important targets for induction of tumor dormancy.

INTRODUCTION

One of the well recognized aspects of tumor progression is the recurrence of cancer in distant sites (metastases) in patients who have undergone curative surgery. Metastases can appear shortly after surgery but can also remain undetected for more than a decade, before manifesting themselves clinically. This indicates that disseminated cancer cells can persist in a dormant state, unable to form a progressively increasing tumor mass. Such heterogeneity of outcome indicates that the fate of tumor cells that disseminate to distant organs before surgery must be regulated by either inherent cancer cell properties or the milieu of the target organs, or both. Identifying the mechanisms that keep metastases in their dormant, occult state is one of the most challenging and important avenues of cancer research.

We reported previously that the tumorigenicity of HEp3 human carcinoma cells is dependent on the interaction of urokinase plasminogen activator (uPA)/uPA receptor (uPAR) complexes with $\alpha5\beta1$-integrin (Aguirre Ghiso *et al.*, 1999b). Because the level of uPAR is high in

* Corresponding author. E-mail: liliana.ossowski@mssm.edu.
Abbreviations used: CAM, chorioallantoic membrane; DMEM, Dulbecco's modified minimal essential medium; IP, coimmunoprecipitation; DAPI, 49,6-diamidino-2-phenylindole; DMSO, dimethylsulfoxide; ECL, enhanced chemiluminescence; ERK, extracellular regulated kinase; FBS, fetal bovine serum; FN, fibronectin; HA-ERK, hemaglutinin-tagged ERK; HRP, horseradish peroxidase; IF, immunofluorescence; IP, immunoprecipitation; MAPK, mitogen-activated protein kinase; P25, peptide 25; p38, p38-MAPK/stress activated protein kinase 2; PBS, phosphate-buffered saline; uPAR, urokinase plasminogen activator receptor.

these cells, the frequency of these interactions is also high, and this leads to activation of the integrin, reflected in an increased adhesion of cells to surface-immobilized fibronectin (FN) and a very strong induction of the extracellular regulated kinase (ERK) 1/2-mitogen-activated protein kinase (MAPK) activity. Strikingly, we showed that down-regulation of uPAR expression in HEp3 cells using antisense technology was sufficient to induce a protracted tumor dormancy with a rapid G_o/G_1 arrest in vivo (Yu *et al.*, 1997; Aguirre Ghiso *et al.*, 1999b). A reduction in uPAR level produced fewer interactions with the $\alpha5\beta1$-integrin, causing the FN-dependent signal to ERK to decrease below a threshold required for in vivo growth and inducing dormancy (Aguirre Ghiso *et al.*, 1999b). Such profound biological change (loss of tumorigenicity) in response to a simple reduction in uPAR level led us to suspect that the disruption of the uPA/uPAR/$\alpha5\beta1$-integrin complex affected additional signaling pathways, in addition to ERK. The stress-activated protein kinase 2 (p38 ^{MAPK}) was a likely candidate because it has been linked to apoptosis and/or growth suppression (Xia *et al.*, 1995; Lavoie *et al.*, 1996; Molnar *et al.*, 1997; Takenaka *et al.*, 1998; Ellinger-Ziegelbauer *et al.*, 1999). Interestingly, one report suggested that p38 activity in fibroblasts is negatively regulated by the presence of surface-associated fibrillar FN (Bourdoulous *et al.*, 1998). We entertained this possibility in spite of the fact that in a majority of published reports oncogenic transformation was shown to be linked to a reduced cell surface FN level (Chandler *et al.*, 1994; Gu and Oliver 1995; Akamatsu *et al.*, 1996; Werbajh *et al.*, 1998). We postulated that, in epithelial tumor cells, uPAR-dependent activation of $\alpha5\beta1$ will lead to assembly of FN fibrils, which will block $p38^{MAPK}$ activity and inhibit this growth-arresting pathway. We set out to test our hypothesis by examining whether HEp3 cells synthesized FN, whether they assemble FN fibrils, and whether a high level of uPAR expression is required for FN fibril assembly by $\alpha5\beta1$-integrin. Here we provide experimental evidence that shows that uPAR, via its regulatory role on FN fibril assembly, can regulate the balance between ERK and $p38^{MAPK}$ activities and that interventions that shift this balance in favor of ERK result in tumorigenicity, whereas those inducing $p38^{MAPK}$ activity induce tumor dormancy.

MATERIALS AND METHODS

Reagents and Antibodies

Dimethylsulfoxide (DMSO), Triton X-100, sodium orthovanadate, NaFl, protease inhibitors DNAse I, bovine serum albumin (BSA), normal goat serum, collagenase type 1A, rhodamine-phalloidin conjugate, human FN, and III1-C fragment of human FN were from Sigma Chemical (St. Louis, MO). Aprotinin and trypsin were from ICN Biomedicals (Aurora, OH). Dulbecco's modified minimal essential medium (DMEM), OPTI-MEM medium, glutamine, antibiotics, and Lipofectin were from GIBCO Laboratories (Grand Island, NY). Fetal bovine serum (FBS) was from JRH Biosciences (Lenexa, KS), COFAL-negative embryonated eggs were from Specific Pathogen-Free Avian Supply (North Franklin, CT), and protein G-agarose beads were from Boehringer Mannheim (Indianapolis, IN). Polyvinylidene difluoride membranes and enhanced chemiluminescence (ECL) detection reagents were from Amersham Life Sciences (Little Chalfont, UK). PD98059, SB203580, and its inactive analogue SB202474 were from Calbiochem (San Diego, CA). The stock solutions were prepared in 100% DMSO. 49,6-Diamidino-2-phenylindole (DAPI) was from Sigma Chemicals. Purified III11-C FN fragment was kindly provided by Dr. Erkki Ruoslahti (The Burnham Institute, La Jolla, CA). Anti-phospho-ERK 1/2 (anti-phospho-Tyr-204; clone E4) and anti-phospho-p38 antibodies were from Santa Cruz Biotechnology (Santa Cruz, CA) and from New England Biolabs (Beverly, MA). Anti-ERK1/2 (clone MK12) and anti-p38 (clone 24) monoclonal antibodies were from Transduction Laboratories (Lexington, KY). Anti-CD29 ($\beta1$-integrin) and anti-CD55/DAF monoclonal antibodies were from NeoMarkers (Union City, CA). Normal mouse IgG, fluorochrome-labeled secondary antibodies, anti-human FN polyclonal antibody (F3648), and anti-FLAG (M2) monoclonal antibody were from Sigma. Goat anti-mouse Alexa-546–conjugated IgG was from Molecular Probes (Eugene, OR). Anti-human uPAR monoclonal antibody R2 was kindly provided by Dr. Michael Ploug (Finsen Laboratory, Copenhagen, Denmark). Rat anti-$\beta1$ and $\alpha5\beta1$-integrin blocking monoclonal antibodies AIIB2 and BIIG2 (Werb *et al.*, 1989), respectively, were kindly provided by Dr. Caroline H. Damsky (University of California, San Francisco, San Francisco, CA), currently available from the Developmental Study Hybridoma Bank (University of Iowa, Ames, IA). Anti-uPAR polyclonal rabbit antibody (399R) was from American Diagnostica (Greenwich, CT). Polyclonal rabbit anti-$\beta1$ antibody (monoclonal antibody 1952) and anti-$\alpha5\beta1$ antibody (clone HA5) were from Chemicon International (Temecula, CA). Anti-mouse IgG monoclonal antibody conjugated with horseradish peroxidase (HRP) and mounting media (Vectashield) were from Vector Laboratories (Burlingame, CA). Anti-rabbit IgG-HRP, anti-mouse IgM-HRP, and anti-HA antibodies (clone 12CA5) were from Boehringer Mannheim (Germany). All antibodies used in vivo or in culture were free of azide. The endotoxin content of antibodies used in culture or in vivo were tested using the Pyrogen-Plus test from Biowhittaker (Walkersville, MD) and were found to have

Cell Lines, Cell Transfections, and Cell Culture Conditions

Human epidermoid carcinoma HEp3 (T-HEp3; Toolan, 1954), serially passaged on chorioallantoic membranes (CAMs), was used as a source of tumorigenic cells (Yu *et al.*, 1997; Aguirre Ghiso *et al.*, 1999b). The source of "spontaneous" dormant tumor cells (D-HEp3) was HEp3 cells passaged in vitro 120–170 times (Ossowski and Reich, 1983) with a uPAR level of only ~20% of that in tumorigenic cells (Aguirre Ghiso *et al.*, 1999b). HEp3 cells transfected with the expression vector LK444 (control, LK25, high uPAR, and tumorigenic) or with LK444 vector expressing antisense uPAR-mRNA (clone AS24, uPAR message and protein reduced by 70–80%, dormant) were described previously (Yu *et al.*, 1997; Aguirre Ghiso *et al.*, 1999b). In addition, D-HEp3 cells were transfected using Lipofectin with 10 μg of pSVNeo plasmid alone or with the same plasmid and a pCMV5 vector encoding a dominant negative mutant of $p38^{MAPK}$ (p38DN; 10 μg), which has a FLAG-epitope tag between codons 1 and 2 (Raingeaud *et al.*, 1995). Stable clones expressing the G418 resistance gene (D-HEp3-neo) or p38DN and antibiotic resistance (D-HEp3-p38DN) were selected with 400 μg/ml G418, pooled to avoid clonal variation, and the pooled population was monitored for FLAG expression by Western blot.

To test the effect of antibodies to uPAR and integrins on in vivo ERK activation, cells were transfected with 5–10 μg of DNA of HA-tagged ERK2 expression vector using Lipofectin according to the manufacturer's instructions as previously described (Aguirre Ghiso *et al.*, 1999b). Twenty-four hours posttransfection, the cells were detached with 2 mM EDTA, incubated with or without 10 μg/ml R2 (anti-uPAR) and 10 μg/ml AIIB2 antibodies at 37°C, and inoculated (2.5×10^6 cell/CAM) into 8-mm-diameter Teflon rings placed on CAMs. After 24 h in vivo, the CAMs were excised and lysed, and the supernatants of cell lysates were analyzed for hema-

glutinin-tagged ERK (HA-ERK) and phospho-HA-ERK by immunoprecipitation (IP) with anti-HA antibodies and Western blotting using anti-phospho-ERK and anti-HA antibodies, as previously described (Aguirre Ghiso *et al.*, 1999b). To test the effect of uPAR expression on ERK activation, D-HEp3 cells were transiently co-transfected with 1 μg of pCDNA3.1 vector and 1 μg of HA-ERK2 plasmid, or HA-ERK2 plasmid and 0.5–2 μg of pcDNA3.1 vector encoding uPAR cDNA, using Fugene transfection reagent (Roche, Gipf-Oberfrick, Switzerland) according to the manufacturer's instructions. HA-ERK phosphorylation was detected as described above.

Growth of Tumor Cells on CAMs

Control T-HEp3, D-HEp3, and AS24 cells, or cells treated with 2–10 μM SB203580 for 48 h, or D-HEp3-neo and D-HEp3-p38DN cells were detached with 2 mM EDTA in PBS, washed, and inoculated on the CAMs of 9- to 10-d-old chick embryos. At different times postinoculation, CAMs were excised and enzymatically dissociated, and single-cell suspensions were counted (Aguirre Ghiso *et al.*, 1999b). In addition, D-HEp3 cells treated with 2 μM SB203580 or D-HEp3-p38DN cells were pretreated in suspension at 37°C for 20 min with 10 μg/ml anti-uPAR antibody (R2) or left untreated, washed, and inoculated onto 10-d-old CAMs. R2 antibody (10 μg/ml) was added to the CAMs after 48 h, and tumor growth was assessed after 4 d and compared with D-HEp3 (DMSO treated) or D-HEp3-neo cells, respectively. Tumor cells were counted in single-cell suspensions as described above. To test the effect of uPAR on the growth of D-HEp3 cells, the cells were transfected with empty pCDNA3.1 vector (2 μg) or with the vector encoding uPAR cDNA (2 μg), and 48 h post-transfection, these cells were inoculated onto 9-d-old chick embryo CAMs. After 7 d of growth in vivo, the number of cells per tumor was determined as described above.

Confocal Laser Scanning and Standard Immunofluorescence (IF) Microscopy

For IF analysis, cells grown on coverslips were fixed with 3% paraformaldehyde in PBS for 15 min. For uPAR, fixing was extended to 30 min (Mayor *et al.*, 1994). The coverslips were washed and either permeabilized with 0.1% Triton X-100 or left nonpermeabilized, washed, blocked with 3% normal goat serum in PBS (15 min), and incubated for 1 h at room temperature with anti-uPAR (R2 at 10 μg/ml), anti-β1-integrin (4B7R, 4 μg/ml), anti-FN (F3648, 1:400), or anti-p38 (clone 24, 1:50) antibodies in 0.1% BSA/PBS or with vehicle alone. After the coverslips were washed and blocked, either the secondary antibodies in 0.1% BSA/PBS containing rhodamine-phalloidin conjugate (1:70) or DAPI was added. Coverslips were mounted in Vectashield and kept at −20°C. Histological sections of tumors obtained from the chick embryo CAM were deparafinized by short heating at 50°C and incubated in xylene twice for 10 min, placed sequentially in 95, 70, and 30% ethanol, for 2 min in each, washed in PBS, and then double-stained for FN and DAPI as indicated above for cells in culture. Standard epifluorescence was captured with an Axioskop epifluorescence photomicroscope (Zeiss, Oberkochen, Germany) using Plan-Neofluar 40 and 100× (NA 1.5 oil) lenses (Zeiss) or a Plan-Apochromat lens 63× (Zeiss) through a SPOT digital camera (Diagnostic Instruments, Sterling Heights, MI) and Photoshop 5.0 software (Adobe, Mountain View, CA). Confocal microscopy was performed using a TCS SP spectral confocal laser scanning microscope (Leica Microsystems, Heidelberg, Germany) equipped with fiber-coupled ultraviolet, visible, and infrared lasers, using Plan-Apo 40, 63, and 100× lenses (NA 1.4 oil). Data were captured and analyzed using the TCS/SP software and Adobe Photoshop 5.0 software.

Detection of Integrin Expression by Fluorescence-activated Cell Sorter (FACS) Analysis

FACS (Becton Dickinson, San Jose, CA) analysis was performed as previously described (Aguirre Ghiso *et al.*, 1999b). Antibodies (HA5, anti-$\alpha5\beta1$, or isotype-matched IgG) were added to 5×10^5 cells at 10 μg/ml and incubated at 4°C for 30 min, followed by two washes and fluorescein isothiocyanate-conjugated goat anti-mouse (1:100 to 1:1000) IgG incubation. Cells were fixed in 5% formaldehyde in PBS and analyzed in FACScan equipped with laser 488. Some cells were treated with 2 μM SB203580 and processed for FACS analysis as described above.

FN Fibril Formation and Effect of Treatments

Cells grown on glass coverslips in DMEM with 10% FBS or 5–10% FN-depleted FBS (Wu *et al.*, 1995), with or without 5–10 μg/ml human serum FN, were fixed and stained for FN and F-actin as indicated above. To test the effect of antibodies or peptide 25 (P25) on FN fibril formation, cells were plated on gelatin-coated (10 μg/ml) coverslips in 5% FN-depleted FBS/DMEM for 1 h, treated with anti-$\alpha5\beta1$ (BIIG2, 20 μg/ml), $\beta1$ (AIIB2, 10 μg/ml) function-blocking antibodies, anti-uPAR antibody to domain III (R2, 10–20 μg/ml), anti-CD55-DAF (15 μg/ml) antibody, or peptide 25 (P25; AESTYHHLSLGYMYTLN-NH2, 5–100 μM), which inhibits uPAR-$\beta1$-integrin interactions (Wei *et al.*, 1996), for 20 min at 37°C, incubated overnight with 5–10 μg/ml human FN, fixed, and stained for FN and F-actin as indicated above. To test the effects of FN fibril disruption by III1-C or III11-C fragments of FN, T-HEp3, or LK25 cells were grown in FN FBS with 5–10 μg/ml FN for 16 h and treated for 16–18 h with III1-C or III11-C fragments (20 μM), or left untreated. The cells were fixed and stained for FN, F-actin, and p38 as indicated above.

The effect of p38 inhibition on FN fibril formation, uPAR, and $\beta1$-integrin surface expression was tested in cells grown for 48 h in DMEM with or without 5% FN-depleted FBS, with or without 10 μg/ml human FN, and/or 2 μM SB203580 or 0.01% DMSO alone as control. Cells were stained for FN and F-actin or for uPAR and $\beta1$-integrin. Nuclei were stained with DAPI. FN fibrils were quantified by counting 200–350 cells per treatment in triplicate experiments and expressed as the percentage of cells with DAPI-positive nuclei.

Detection of Extracellular Matrix-associated FN by Deoxycholate Extraction

Cells grown for 24 h in DMEM with FBS were lysed for 20 min at 4°C with 3% Triton X-100, 10 μM EDTA in PBS, and protease inhibitors and centrifuged, and the supernatants were used for determination of protein concentration. Triton-insoluble pellets were treated with 100 μg/ml DNAse in 50 mM Tris, pH 7.4, 10 mM $MnCl_2$ for 20 min at room temperature. Then, 2% deoxycholate in 50 mM Tris, pH 8.8, and 10 mM EDTA were added, and the mixture was centrifuged for 15 min at 14,000 rpm. The insoluble and soluble fractions were mixed with sample buffer with or without 100 mM β-mercaptoethanol, analyzed on 6% SDS-PAGE, and tested by Western blotting using polyclonal anti-human FN antibodies and ECL for detection.

Adhesion Assays

The method used was essentially as previously described (Aguirre Ghiso *et al.*, 1999b) except that cells were treated for 48 h with 2 μM SB203580 or 0.01% DMSO, before being detached with 2 mM EDTA, inoculated (50 μl per 96-well tray) into wells coated with increasing concentrations of FN, incubated for 10–30 min, fixed, and stained.

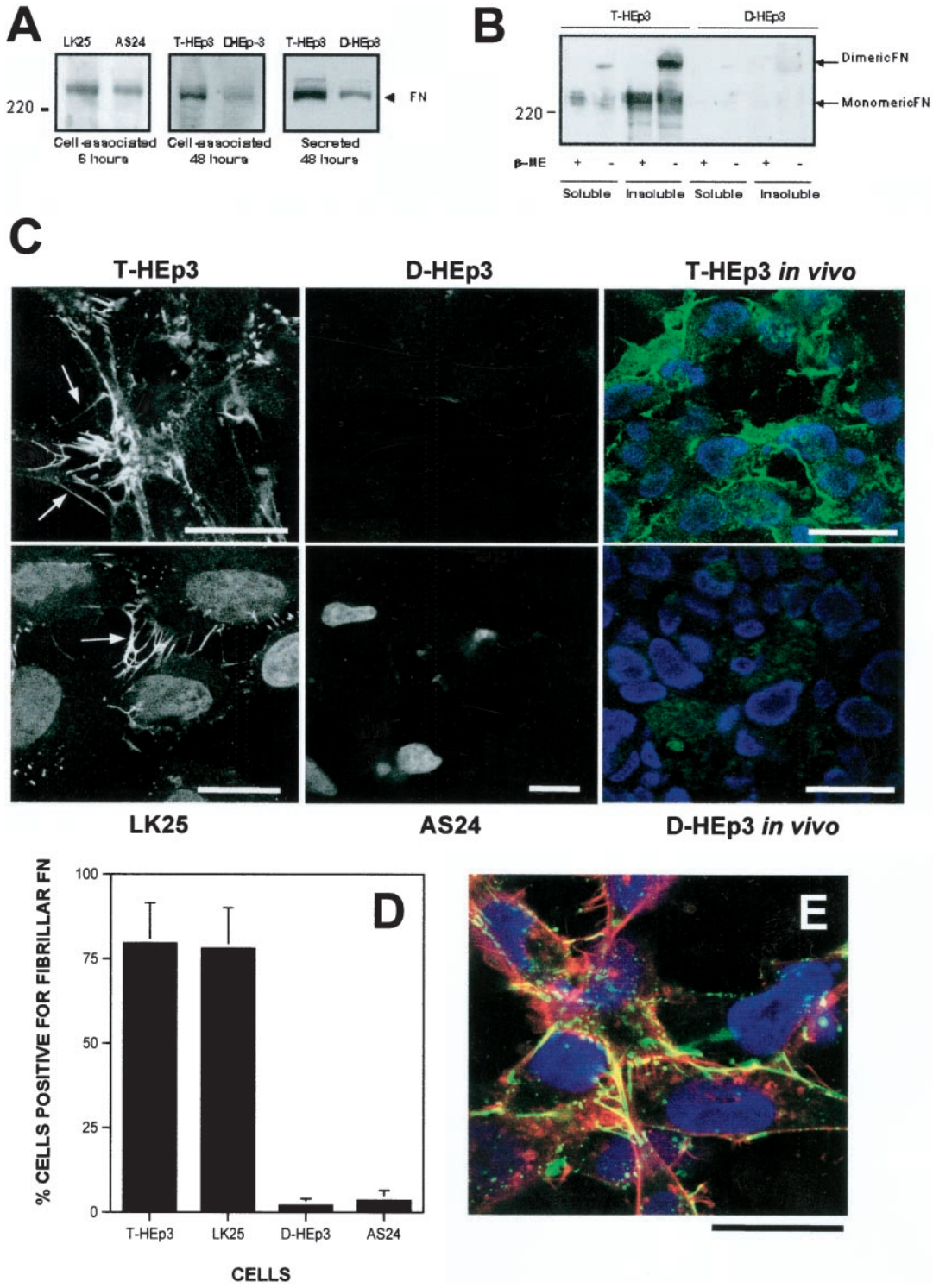

Figure 1. Production and extracellular organization of FN in tumorigenic and dormant HEp3 cells. (A**)** Total cellular FN of cells grown in FN-depleted FBS for 6 h (left) and 48 h (middle) and lysed or secreted FN (right) were determined by SDS-PAGE under reducing conditions and Western blot. The arrow indicates monomeric FN. LK25 and T-HEp3 tumorigenic cells; AS24 and D-HEp3 dormant cells (see MATERIALS AND METHODS). (B**)** Western blot of insoluble FN matrix. Deoxycholate-soluble and -insoluble fractions (50 μg of protein) of T-HEp3 and D-HEp3 cells were separated by SDS-PAGE under reducing or nonreducing conditions and tested for FN by Western blotting. β-ME, β-mercaptoethanol. The arrows indicate dimeric or monomeric FN. (C**)** Confocal laser scanning IF (XY sections) for FN. Tumorigenic (T-HEp3/LK25) cells or dormant (D-HEp3/AS24) cells were plated in FN-depleted FBS supplemented with 5 μg/ml human FN and, after 16 h**,** fixed and stained with anti-human FN antibody. The arrows indicate FN fibrils that appeared

Northern Blot Analysis

Total RNA from ~1 × 10^7 D-HEp3 cells untreated or treated with SB203580 for 5, 16, 24, and 48 h, was extracted using an Ultraspec RNA isolation system (Biotecx Laboratories, Houston, TX), 50 μg of RNA was transferred to Hybond nylon membranes (Amersham Life Sciences, Buckinghamshire, England), cross-linked with UV light, incubated overnight with a ^{32}P-labeled 1.4-kb uPAR-cDNA probe labeled using random priming (DECA prime II DNA labeling kit, Ambion, Austin, TX). Stripped membranes were reprobed with 36B4 ribosomal protein cDNA, as a loading control labeled with a nonisotopic method (psoralen-biotin, Bright Star, Ambion). The signal was developed using XOMAT film (Kodak, Rochester, NY) with intensifying screens after exposure for 4–24 h at −80°C. The bands were quantitated using a laser scanner densitometer (GelScan XL, Pharmacia, Uppsala, Sweden).

Detection of ERK and p38^{MAPK} Activation

Cell lysates of subconfluent monolayers were prepared as previously described (Aguirre Ghiso *et al.*, 1999b) and centrifuged, and equal amounts (60 μg) of the supernatant proteins were used in Western blots to detect either active or total ERK and p38 levels using phospho-ERK (p42/p44) or phospho-p38 antibodies or ERK1 or p38 Antibodies. Alternatively, basal levels of active-p38 were determined by IP with anti-phospho-p38 antibodies and blotting with anti-p38 antibodies(see below). The effect of p38 inhibition on ERK activation was tested by treating the cells with 1–10 μM SB203580 or its inactive analogue SB202474 or 0.05% DMSO, for 5–20 min or 5–48 h in serum-free DMEM. In some experiments, after 48 h of treatment, the inhibitor was washed out and the cells were cultured for an additional 24–72 h in serum-free medium. In some experiments, 2 μM SB203580 was added to cell monolayers in the presence of the Mek inhibitor PD98059 (30 μM), and ERK activation levels were detected. The phospho-ERK and ERK levels were analyzed by Western blotting. Phospho-ERK and ERK levels were also detected in D-HEp3-neo or D-HEp3-p38DN cells as described previously. FLAG expression was checked in all experiments to verify p38-DN expression. To test the effect of disrupting the uPAR/β1-integrin complex on p38 activation, cells were plated on gelatin (10 μg/ml)-coated plates in FN-depleted serum for 1 h at 37°C, incubated with anti-uPAR (10 μg/ml), anti-α5β1 (20 μg/ml), or anti-β1 (10 μg/ml) antibodies for an additional 20 min, and supplemented with 10 μg/ml human FN. The cells were incubated overnight and lysed, and the soluble fraction (400 μg) was subjected to IP with anti-P-p38 antibodies (Santa Cruz) for 1 h at 4°C. The immunocomplexes were incubated for 1 h at 4°C with secondary antibody-conjugated protein G-beads, and after SDS-PAGE, and transfer, the membranes were blotted with anti-p38 monoclonal antibody and the signal was developed using ECL.

Figure 1 (facing page). to be mostly apical but also basolateral and in many cases formed cell-cell bridges. Staining for FN and visualization of nuclei was also performed on histological sections of T-HEp3 or D-HEp3 cells maintained in vivo on the CAM for a week (right). Note the absence of FN matrix deposition in dormant cell lines in culture and in vivo. (D) Quantitation of FN fibril-positive cells. Cells were double-stained with anti-FN antibodies (as in C) and with DAPI. The number of FN fibril-positive cells is expressed as a percentage of DAPI-stained cells. (E) Colocalization of FN and F-actin by confocal IF microscopy. LK25 cells were grown as in C and, after fixing, triple-staining for FN (green), F-actin (red), and nuclei (blue) was performed. The yellow signal indicates colocalization of FN and F-actin. Note that the fibrillar or globular FN colocalizes with the F-actin cytoskeleton and that FN fibrils extend beyond the cell body (see also Figure 2A). The images in C and E are representative of the most prevalent cell types. Bars, 40 μm.

Effect of SB203580 on uPAR, FN, β1-Integrin, and ERK Expression

D-HEp3, AS24, and T-HEp3 cells cultured for 24 h in 10% FBS/DMEM were washed twice with serum-free medium and treated with SB203580 (2–4 μM) or its inactive analogue SB202474 (4 μM) in 0.01% DMSO or 0.01% DMSO alone. At different times, cells were scraped and lysed with the appropriate buffers and Western blotted with antibodies anti-uPAR, β1-integrin, or ERK. Expression of uPAR was also detected by Western blot in D-HEp3 cells treated with control media, 2 μM SB203580 or 2 μM SB203580 plus 30 μM PD98059 or in D-HEp3-neo and D-HEp3-p38DN cells as described above. For FN detection, cells were trypsinized (to remove FN bound to cells), plated, and grown in media containing 5% FN-depleted FBS or medium alone containing 2 μM SB203580. After 6, 24, and 48 h the cells were lysed with modified RIPA buffer, and the soluble fraction was used for Western blotting with polyclonal rabbit anti-FN antibodies.

IP of α5β1-Integrin and Detection of uPAR

D-HEp3 cells, untreated or treated with 2 μM SB203580 alone or in combination with PD98054, were lysed and extracted for 1h with a lysis buffer containing 1% Triton X-100, 50 mM HEPES, pH 7.5, 150 mM NaCl, 1 mM $CaCl_2$, 1 mM $MgCl_2$, 1 mM orthovanadate, 1 mM NaFl, and protease inhibitors. Triton X-100-insoluble fractions (400 μg of protein) were extracted for 30 min with modified RIPA lysis buffer and incubated with 4 μg of anti-α5β1 (HA5) or matched isotype IgG overnight at 4°C, precipitated with protein G-agarose beads and washed three times. The beads were resuspended in 2× Laemmli sample buffer, heated to 95°C for 10 min, and analyzed by Western blotting using anti-β1-integrin (anti-CD29) polyclonal antibodies or anti-uPAR 399R polyclonal antibodies.

RESULTS

We have previously shown that interaction of uPA/uPAR with the α5β1-integrin leads to activation of the integrin, greatly enhanced adhesion of cells to immobilized FN, and ERK activation in vitro and in vivo. Because one of the consequences of α5β1-integrin activation is its ability to assemble soluble FN into fibrils, we tested whether tumorigenic HEp3 cells with high uPAR levels possessed this ability and whether the presence of uPAR-regulated FN fibrils affected the levels of active MAPK signalling and tumorigenicity.

FN Expression and Fibril Formation by uPAR-rich, Tumorigenic and uPAR-deficient Dormant Cells

FN production by both types of cells was measured using Western blotting analysis of equal amounts of RIPA-cell lysate proteins or conditioned media of cells grown in FN-depleted serum. Both tumorigenic and dormant cells produced FN. The level of cell-associated FN protein at 6 and 48 h (Figure 1A, left and middle) and secreted FN (Figure 1A, right) was somewhat lower in dormant cells, but even these cells secreted ~4 μg of FN per ml in 48 h. However, whereas most of the dormant cell FN was secreted (Figure 1B), much of the FN produced by tumorigenic cells was cell-associated and deoxycholate insoluble (Figure 1B), indicating that it is organized into matrix fibrils (Wu *et al.*, 1995). In confirmation, FN staining and IF analysis of fixed, nonpermeabilized T-HEp3 and LK25 cells (tumorigenic, with high uPAR) showed well organized extracellular FN fibrils, many apical, but some basolateral, whereas the D-HEp3 or

AS24 cells (dormant, with low uPAR) had very few fibrils (Figure 1C). Moreover, in histological sections of T-HEp3 tumors grown on the CAMs of chick embryos and stained with anti-FN antibodies, the tumor cells were surrounded by FN organized into fibrils. In contrast, in sections of D-HEp3 cells maintained on the CAM, FN appeared to be homogeneously distributed throughout the stroma with no evidence of organization (T-HEp3 and D-HEp3 in vivo, Figure 1C). The count of FN fibril-positive cells in culture showed only 1–2% in the D-HEp3 and AS24, and ~80% positive cells in T-HEp3 and LK25 cultures (Figure 1D). In nonpermeabilized tumorigenic cells, the FN fibrils colocalized with actin filaments (Figure 1E), often in the leading edges, filopodia, or lamelipodia, and frequently extending beyond F-actin and beyond the cell body limits, in a mesh-like structure (Figure 1E). An abundance of fibrils, colocalizing with F-actin, was also found in cell-cell contacts. The F-actin in these cells was predominantly cortical, with no evidence of stress fibers (Figure 1E).

We previously showed that $\alpha5\beta1$-integrin and uPAR can be coprecipitated from the Triton X-100-insoluble fraction of cell-surface biotinylated HEp3 cells, suggesting that these proteins form a cell surface complex (Aguirre Ghiso *et al.*, 1999b). To test whether FN fibril formation by tumorigenic cells was dependent on uPAR and its interaction with the integrin, cells plated on gelatin-coated coverslips were treated either with antibodies to domain III of uPAR or with a peptide (p25) known to disrupt the $\alpha5\beta1$/uPAR interaction and signaling (Wei *et al.*, 1996; Aguirre Ghiso *et al.*, 1999b). In addition, blocking antibodies to $\alpha5\beta1$ or to $\beta1$ were used to disrupt fibrils, whereas untreated cultures or cultures treated with antibodies to CD55 (an antigen expressed on the surface of HEp3-cells; Aguirre Ghiso *et al.*, 1999b) served as controls for FN fibril formation. Most cells (~80%) in untreated or anti-CD55 antibody-treated cultures were able to assemble FN fibrils (Figure 2, A, a and e, and B), whereas anti-$\beta1$ and $\alpha5\beta1$ antibodies blocked their assembly, leaving only <5 and <20% of FN fibril-positive cells, respectively (Figure 2, A, b and c, and B, left). More importantly, both peptide 25 and anti-uPAR antibody reduced the proportion of FN fibril-positive cells to <25% (Figure 2, A, d and f, and B, left and right), supporting the idea that uPAR, through its interaction with $\alpha5\beta1$-integrin, regulates cell ability to organize FN fibrils.

Does Blocking of FN Fibril Assembly in Tumorigenic Cells Change Their Intracellular Signaling?

A published report (Bourdoulous *et al.*, 1998) suggested a link between the lack of FN fibrils in fibroblasts and endothelial cells and activation of Cdc42 and p38 ^{MAPK}. We wondered whether a consequence of the lack of FN fibrils in dormant cells is also activation of p38 ^{MAPK}. To test this, lysates of dormant D-HEp3 or AS24 cells and tumorigenic T-HEp3 and LK25 cells were examined for active p38 (P-p38) either by direct blotting with antibodies to P-p38 (Figure 3A) or by IP with the anti-P-p38 antibodies and Western blotting with anti-p38 antibodies (Figure 3B). The level of active p38 was four- to fivefold greater in the dormant cells and, compared with the tumorigenic cells, the ratio of active p38 to active ERK (Figure 3A, right) was inverted. Moreover, fibril-blocking treatments of T-HEp3 and LK25 cells plated for adhesion on gelatin-coated dishes, incubated for 12 h in medium with 10 μg/ml human FN and anti-uPAR, anti-$\alpha5\beta1$, or anti-$\beta1$ antibodies, respectively, produced an approximately fourfold induction in p38 activity. The level of active p38 in untreated cultures was always slightly higher in LK25 than in T-HEp3 cells (Figure 3, A–C), but in each case disruption of FN fibrils caused a strong induction in p38 activity (Figure 3C). (Disruption of fibrils with anti-$\beta1$-integrin antibodies always produced two bands [Figure 3C], most likely because of activation of an additional p38 isoform.). The well organized FN fibrils in LK25 cells (Figure 3D, a) could also be disrupted by 16-h treatment of the cells with a high concentration of the first type III repeat of FN (III-1C) (Bourdoulous *et al.*, 1998) but not with an inactive FN fragment (III-11C; Figure 3D, b and c, respectively). Disassembly of fibrils led to a reorganization of the predominantly cortical actin cytoskeleton into filopods (results not shown) and translocation of p38 from the cytoplasm into the nucleus (Figure 3D, e), suggesting its activation as previously reported (Cheng and Feldman, 1998). Therefore, a pathway of p38 activation can be induced in highly tumorigenic cells simply by blocking the uPAR/integrin interaction and FN fibril formation. These results posed new questions relating to the contribution of p38 signaling to the induction of the dormant phenotype, as well as its effect on ERK pathway activity.

p38 Activation Negatively Regulates the ERK Pathway in Dormant Cells

To test for cross-talk between the p38 and ERK activities, D-HEp3 and T-HEp3 cells were incubated with 2 or 5 μM of SB203580, shown to specifically inhibit the activity of α and β isoforms of p38 (Enslen *et al.*, 1998; Eyers *et al.*, 1998). An increase in ERK activity to a level similar to the basal level in T-HEp3 cells (Figure 4A, left) was observed in D-HEp3 cells within 5 min of SB203580 treatment, (Figure 4A, right), whereas inhibitor-treated T-HEp3 cells responded with a mild stimulation (Figure 4A, left). The initial activation of ERK was sustained for 5 h, beyond which time a further 10-fold increase in active ERK occurred that was maintained for 48 h of treatment and for 72 h after the inhibitor was washed out (Figure 4B). In the AS24 cells, only the initial, rapid activation of ERK was seen at any time point tested (Figure 4C). To confirm these results by a genetic approach, D-HEp3 cells were stably transfected with a FLAG-tagged dominant negative p38-coding construct, or vector control, and stable, G418-resistant transfectants were selected. ERK activation in cells expressing the dominant negative p38 protein increased to the level found in the tumorigenic HEp3 cells and was much higher than the level found in vector-transfected D-HEp3 cells (Figure 4D).

Inhibition of p38 Induces uPAR Expression and Restores Its Surface Colocalization with the β1-Integrin

Overall, the above results suggest two levels of cross-talk between p38 and ERK, one immediate, and most likely regulated by a phosphorylation cascade, and a second delayed, more pronounced and most likely involving synthesis of new proteins. Because transcription of both uPAR and uPA was shown to be positively regulated by the Raf-MEK-ERK pathway (Lengyel *et al.*, 1997; Aguirre Ghiso *et al.*,

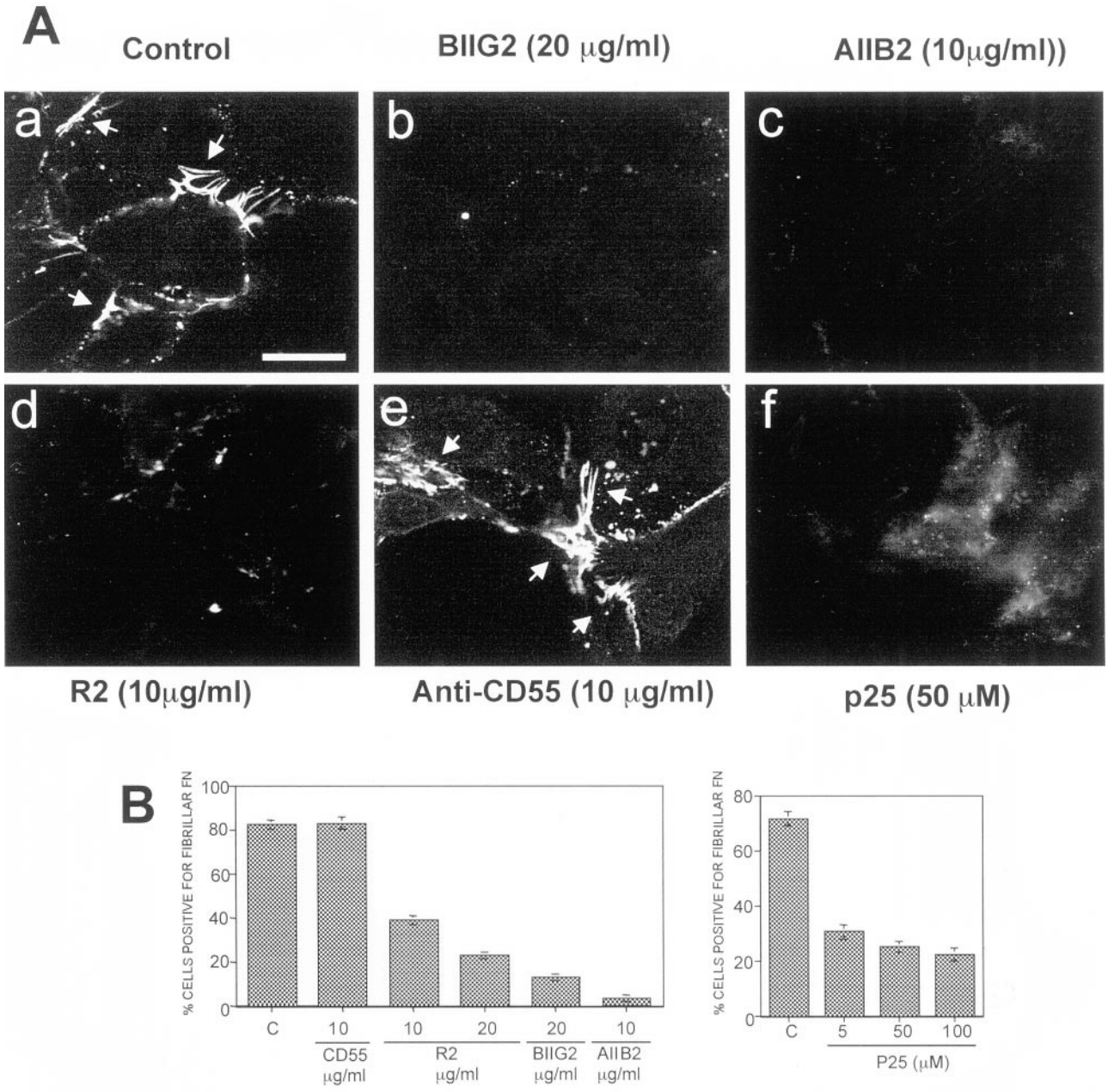

Figure 2. The effect of disruption of uPAR-integrin association on FN fibrillogenesis. (A) LK25 cells plated on gelatin (10 μg/ml)-coated coverslips for 60 min were preincubated with medium alone (a) or with antibodies to $\alpha5\beta1$-integrins (BIIG2 20 μg/ml, b), $\beta1$-integrin (AIIB2 10 μg/ml, c), uPAR (epitope in domain-III, R2, 10 μg/ml, d), CD55 (CD55/DAF, 15 μg/ml, e), or medium with 50 μM peptide p25 (f), for 20 min (AIIB2 and BIIG2 are function-blocking antibodies). Human FN (5 μg/ml) was then added to all wells, and the cells were incubated overnight to allow for FN fibrillogenesis. Cells were examined by IF confocal laser scanning microscopy. The arrows indicate FN fibrils between or beyond cell bodies. (B) Quantitation of FN fibril-positive cells. At least 200 cells were scored per treatment in duplicate. Treatments in the left graph are: C, control medium; CD55, antibody anti-CD55 (10 μg/ml); R2, uPAR antibody (10 and 20 μg/ml); BIIG2, anti-$\alpha5\beta1$ antibody (20 μg/ml); AIIB2, anti-$\beta1$ antibody (10 μg/ml). Treatments in right graph are: P25, peptide 25 that disrupts uPAR-integrin interaction (5, 50, and 100 μM). Quantitation of FN fibril-positive cells was performed as described in Figure 1, C and D, using DAPI staining. Bar, 40 μm

1999a), we speculated that the first wave of ERK activity may lead to uPAR re-expression that, in turn, may initiate the second permanent and strong wave of ERK activation (Figure 4B).

Thus, D-HEp3 cells treated for different periods of time with 2 μM SB203580 were tested for uPAR-mRNA content by Northern blot analysis. UPAR-mRNA level was increased at 5 h of treatment and remained elevated for at least

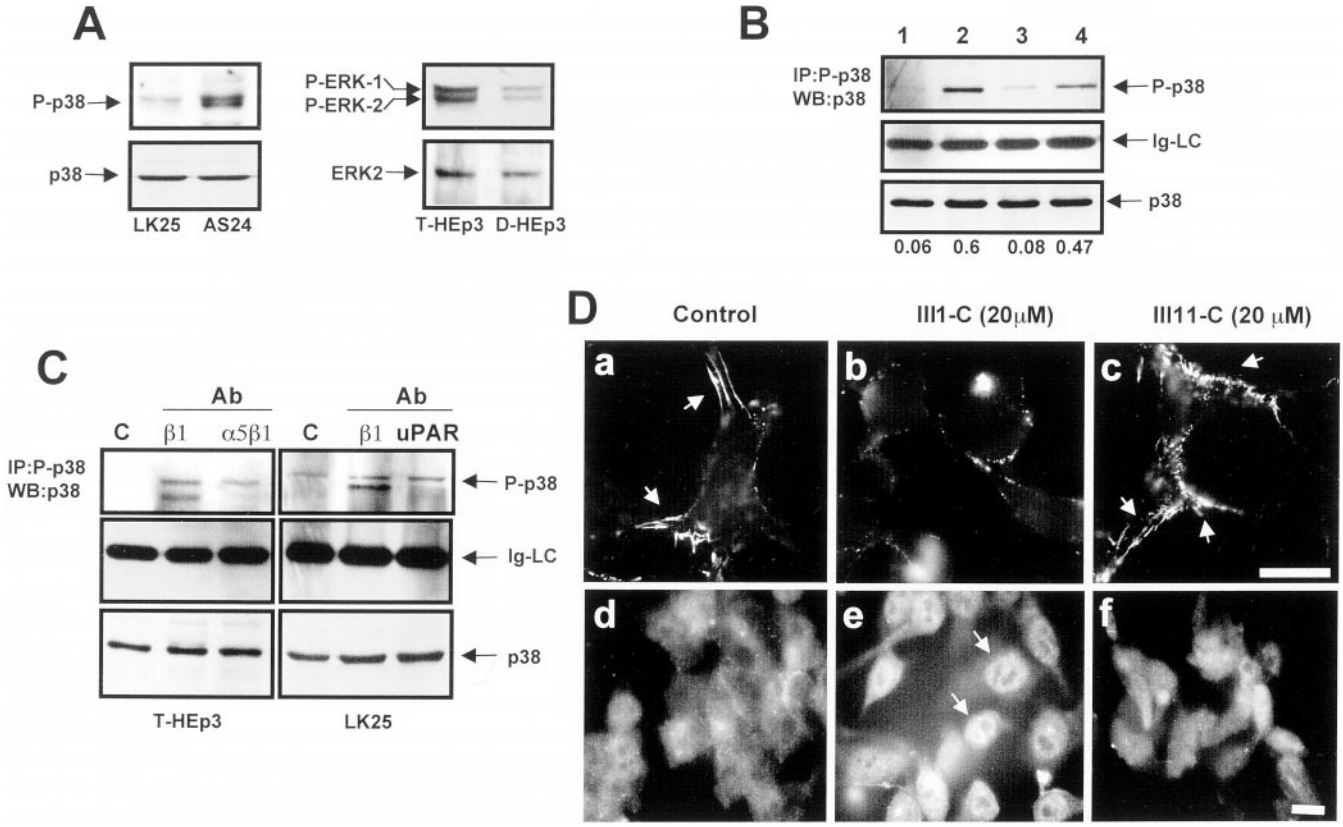

Figure 3. Disruption of FN fibrillogenesis alters the p38/ERK activity ratio. (A) Basal levels of active and total p38 in LK25 and AS24 cells, serum-starved for 24 h (left) or basal levels of active and total ERK in T-HEp3 and D-HEp3 cells serum-starved for 24 h (right) were detected by Western blotting using anti-phospho-p38 (P-p38) and p38 antibodies (p38) or anti-phospho-ERK (P-ERK1/2) and anti-ERK (ERK2) antibodies. (B) Active p38 in T-HEp3 (lane 1), D-HEp3 (lane2), LK25 (lane3), or AS24 (lane 4) cells was detected by IP with anti-phospho-p38 antibodies and blotting with anti-p38 antibodies (top, P-p38). Middle, light chain of IgG (Ig-LC), as a gel-loading control. Bottom (p38), total p38 in cell lysates used for IP as detected by Western blotting. The numbers below each lane show the P-p38 to p38 ratio. (C) Effect of blocking FN fibrillogenesis or disruption of uPAR-integrin complex on p38 activation. Cells were plated in gelatin-coated dishes and treated with anti-β1 or anti-$\alpha5\beta1$ antibodies as indicated in Figure 2A (T-HEp3, left) or with anti-β1 and anti-uPAR antibodies (LK25, right). The cells were lysed and active p38 was detected as in B. c, control (no antibody); cells treated with antibodies to: β1 (AIIB2, 10 μg/ml), $\alpha5\beta1$ (BIIG2, 20 μg/ml), or uPAR (R2, 10 μg/ml). Control LK25 cells always displayed a slightly higher level of active p38 than T-HEp3 cells (see B and C). (D) Effect of FN fibrils disruption with FN III1-C fragment on p38 activation. LK25 cells were plated in FN-depleted FBS supplemented with 5 μg/ml human FN. After overnight incubation to allow for FN fibrillogenesis, the cells were left untreated (control, a and d) or were treated for 16 h with 20 μM III1-C (b and e) or III11-C (c and f) fragments of FN. Cells were then fixed and stained for either FN (a–c) or with anti-p38 monoclonal antibodies (d–f) and visualized by standard IF. The arrows indicate FN fibrils present only in untreated or control (III11-C) -treated cells (a and c) or p38 in the nucleus (e) after FN fibrils disruption with III1-C FN fragment. Bars, 40 μm.

48 h (Figure 5A). uPAR protein level increased slightly at 5 h but was elevated approximately fourfold over control at 16 h and remained elevated for up to 48 h (Figure 5B). SB203580 treatment had no effect on uPAR expression in T-HEp3 cells (results not shown). An inactive analogue of the p38 inhibitor, SB202474, did not increase ERK activity or the level of uPAR protein, indicating the specificity of the effect of the p38 inhibitor (results not shown). Moreover, in AS24 cells expressing antisense to uPAR message and treated with the p38 inhibitor, there was neither a second wave of ERK activation (Figure 4C) nor an increase in uPAR protein, presumably because sufficient uPAR antisense RNA has been present to block the newly transcribed uPAR-mRNA (results not shown). A similar increase in uPAR expression was found in D-HEp3 cells stably transfected with a dominant negative form of p38 (Figure 5C), which also had high ERK activity (Figure 4D). To test whether the increase in uPAR level subsequent to p38 inhibition was mediated through ERK activation, control D-HEp3 cells and cells treated with SB203580 alone or with the combination of SB203580 and MEK inhibitor (PD98059) were examined for active ERK and uPAR levels. As shown in Figure 5D, the induction of active ERK and re-expression of uPAR achieved through p38 inhibition were both abrogated by the addition of MEK inhibitor. In contrast, neither the level of β1-integrin, determined by Western blot (results not shown) nor the level of $\alpha5\beta1$ determined by FACS analysis, was changed in D-HEp3, AS24, or T-HEp3 cells when p38 was inhibited (Figure 5E). Moreover, the amount of uPAR that coimmunoprecipitated with the $\alpha5\beta1$-integrin from D-HEp3 cells in which

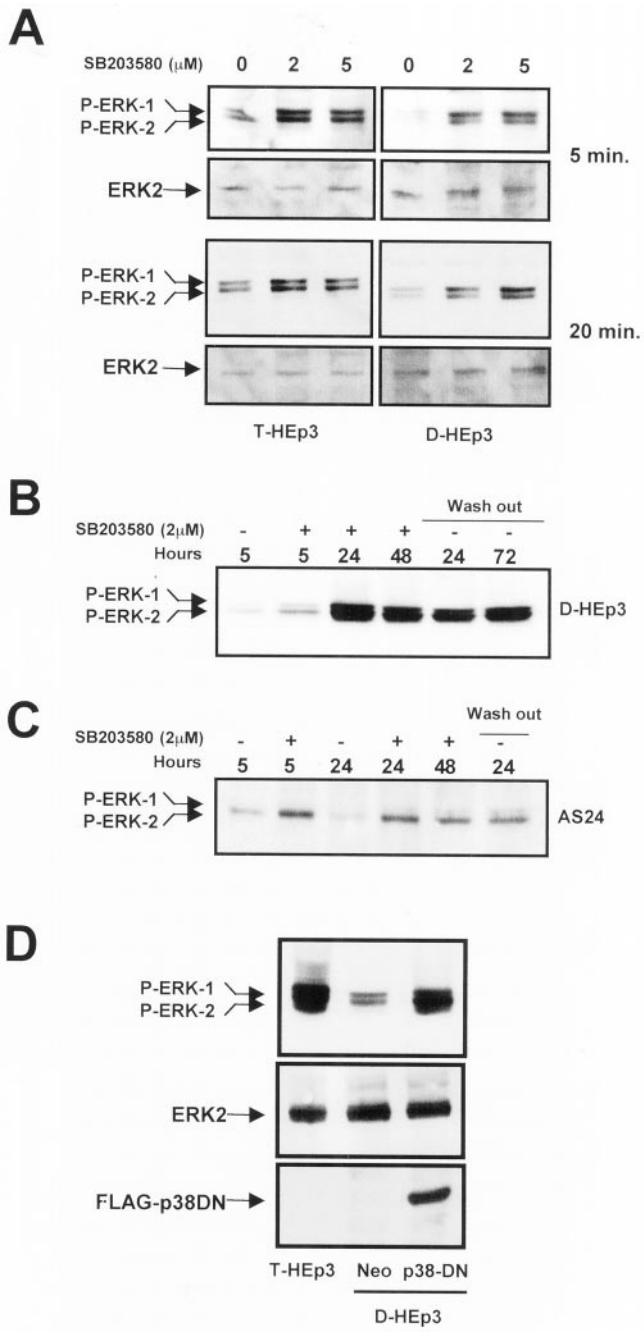

Figure 4. Analysis of cross-talk between ERK and p38 pathways. (A) Effect of p38 inhibition on ERK activation (short-term treatment). Serum-starved T-HEp3 (left) or D-HEp3 (right) cells were treated for 5 or 20 min with 0, 2, and 5 μM SB203580 in DMSO, then lysed, and assayed by Western blotting using anti-phospho-ERK for active ERK or anti-ERK antibodies for total ERK. (B) Long-term treatment. D-HEp3 cells were treated in the absence of serum for 5, 24, and 48 h with 2 μM SB203580 (+) or DMSO (−) and assayed after lysis for ERK activation as indicated in A. After 48 h of treatment some cultures were washed free of the inhibitor and incubated for an additional 24 and 72 h in serum-free medium (lanes indicated as wash-out) before lysing and testing for active ERK. (C) AS24 cells were treated as in B: DMSO treated (−) for 5 or 24 h or SB203580 treated (+) for 5, 24, and 48 h; some plates were treated with the inhibitor for 48 h, washed, and incubated in serum-free medium for an additional 24 h (wash out). (D) Effect of the stable expression of a dominant negative p38 on ERK activation. Pools of D-HEp3-neo or D-HEp3-p38DN cells were lysed and the levels of active and total ERK, as well as the levels of FLAG protein, were detected by Western blotting as in A and compared with the level of active ERK in parental, tumorigenic T-HEp3 cells.

p38 was inhibited by SB203580 was much greater than the amount in cells treated with SB203580 and an inhibitor of MEK or untreated (Figure 5F). The colocalization of uPAR synthesized in response to p38 inhibition with the β1-integrin was tested also by confocal IF. T-HEp3 and D-HEp3 cells, control and p38 inhibitor treated (Figure 6, A, D, and G, respectively), expressed similar amounts of surface β1-integrin. However, whereas T-HEp3 cells had a strong signal for membrane-localized uPAR (Figure 6B), D-HEp3 cells had an almost undetectable signal (Figure 6E). In response to p38 inhibition, D-HEp3 cells re-expressed uPAR, which was localized to both the apical and the basolateral plasma membrane (Figure 6H), and as in T-HEp3 cells (Figure 6C and inset) the newly synthesized receptor colocalized with the β1-integrin on the surface of cells (Figure 6I and inset). These results indicate that in dormant cells an active p38 pathway negatively regulates ERK activity and uPAR expression. When the p38 pathway is inhibited, it allows uPAR re-expression and a permanent strong ERK activation.

Inhibition of p38 and Re-Expression of uPAR Restore the High Affinity of α5β1-Integrin and FN Fibrillogenesis

We showed previously that high uPAR expression increases cell adhesion to immobilized FN (Aguirre Ghiso *et al.*, 1999b). Here we show that treatment of D-HEp3 cells with 2 μM SB203580 for 48 h, which induces uPAR (Figures 5 and 6), also results in enhanced cell adhesion to FN; the strongest stimulation of adhesion was observed at the lowest (0.5 μg) concentration of FN (Figure 7A). A short treatment with the inhibitor did not cause an increase in adhesion to FN (results not shown), suggesting that increased uPAR expression is required for integrin activation and function.

Dormant cells treated with the p38 inhibitor acquired the ability to form FN fibrils. Confocal microscopy of D-HEp3 and AS24 cells incubated for 48 h in FN-depleted serum with or without 5 μg/ml human FN, as previously, revealed very few cells with FN fibrils (Figure 7, B, a and d, and C). In contrast, in D-HEp3 cells treated with 2 μM SB203580 inhibitor, ~25% cells were positive for FN fibrils (Figure 7, B, b, and C). The increase in FN fibril content was not simply due to increased FN synthesis, because Western blot analysis of SB-treated cells, grown in absence of exogenous FN, showed no increase in total FN content (results not shown). A further increase in the percentage of cells with fibrils was found when 5 μg/ml FN was added to the cultures (Figure 7, B, c, and C), but even these fibrils were somewhat shorter and smaller in diameter than in T-HEp3 cells, suggesting that additional factor(s) may be required. To show that uPAR was the regulator of fibrillogenesis in cells treated with p38 inhibitor, we expressed uPAR in D-HEp3 cells directly by a transient transfection. These cells, which by Western blotting

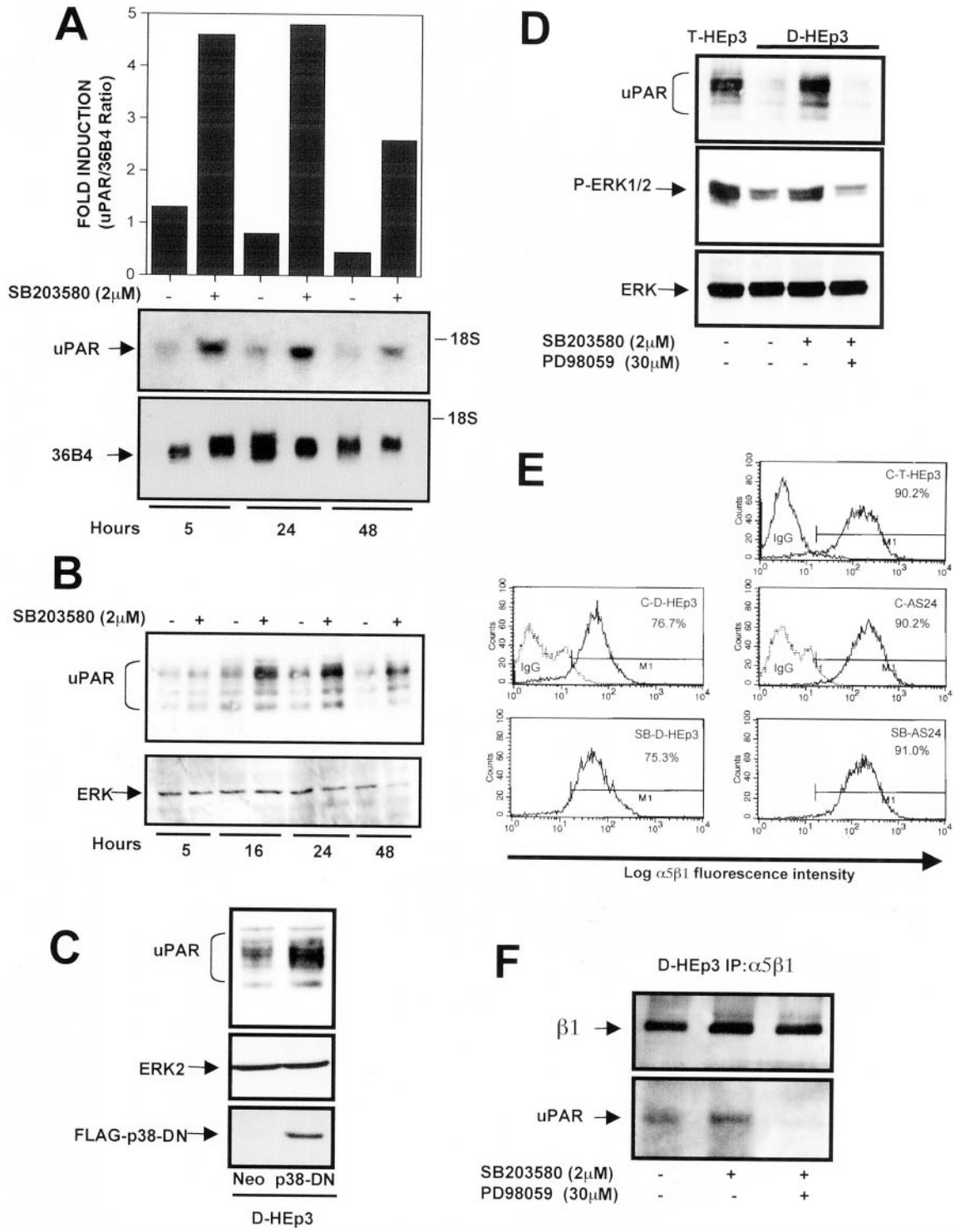

Figure 5. Effect of p38 inhibition on uPAR and $\alpha 5\beta 1$ expression (A) uPAR-mRNA level. RNA extracted from D-HEp3 cells treated with DMSO (−) or 2 μM SB203580 in DMSO (+) for 5, 24, and 48 h were tested by Northern blot using ^{32}P-labeled uPAR-cDNA as a probe. Bottom, 36B4 mRNA used as a loading control. The graph shows the ratio of uPAR/36B4 signals, measured by laser scanning densitometry. (B) uPAR-protein level. D-HEp3 cells were incubated with 2 μM SB203580 in DMSO (+) or DMSO (−) for 5, 16, 24, or 48 h and, after lysis, the cells were processed and analyzed by Western blotting for uPAR. Total ERK served as a loading control. (C) uPAR protein levels in cells expressing a dominant negative p38. D-HEp3-neo or D-HEp3-p38DN cells were lysed and the levels of uPAR, ERK (as loading control), or p38DN were detected by Western blot. (D) Effect of Mek inhibition on SB203580-induced ERK activation and uPAR up-regulation. D-HEp3

analysis showed a very high level of uPAR protein (Figure 8B), produced easily distinguishable surface FN fibrils (Figure 7B, e and f), whereas no fibrils were observed in vector-transfected D-HEp3 cells. In AS24 cells, in which there is no increase in uPAR protein level after p38 inhibition, the number of cells with FN fibrils increased only threefold as opposed to ~25 fold in D-HEp3 cells (Figure 7C).

Inhibition of the p38 Pathway Interrupts Dormancy in D-HEp3 by Inducing uPAR Expression

Our previous results (Aguirre Ghiso *et al.*, 1999b) have shown that the association of uPA/uPAR/$\alpha5\beta1$ proteins enhances cell adhesion to FN and stimulates ERK activity. We also showed that treatment of cells in culture with antibodies that disrupt the interaction of $\beta1$-integrin with uPAR caused a reduction in ERK activity that translated into a state of transient dormancy upon inoculation of these cells on CAMs. Now we show that the uPAR/integrin interaction activates $\alpha5\beta1$-integrin sufficiently to facilitate FN fibril formation, leading to suppression of p38 activity and altering the balance between active ERK and p38. To test whether the ratio of active ERK to p38 was indeed responsible for the in vivo behavior of HEp3 cells, and whether uPAR level was the regulator of these events, we performed several experiments. First, tumorigenic T-HEp3 or LK25 cells were transfected with an HA-ERK construct, incubated in suspension with anti-$\beta1$-integrin and anti-uPAR antibodies, or without antibodies, and inoculated on 9-d-old CAMs. Twenty-four hours after the inoculation, tumor cells were recovered and analyzed for HA-ERK and phospho-HA-ERK content. We found (Figure 8A) that pretreatment with the antibody produced a two to -threefold reduction in ERK phosphorylation in vivo, a result that fits well with the inability of these cells to form tumors after the same treatment (Aguirre Ghiso *et al.*, 1999b). Conversely, when uPAR poor, D-HEp3 cells were transfected with a uPAR-coding construct, they expressed a high level of uPAR protein and showed persistent activation of ERK (Figure 8B, top). The increase in ERK activation was proportional to the amount (0.5–2.0 μg) of uPAR-construct DNA used for transfection (Figure 8B, bottom), as determined by cotransfection with uPAR/HA-ERK constructs. This dose dependence provided an additional link between uPAR level and ERK activation. Moreover, we showed that re-expression of uPAR by transient transfection of D-HEp3 cells, relieved their in vivo growth arrest, allowing the cells to proliferate on the CAMs (Figure 8C). Similarly, D-HEp3 cells in which uPAR expression and uPAR/integrin signaling to ERK (Figure 4, A and B), as well as FN fibril formation, was increased through p38 inhibition with SB203580 (2 μM for 48 h), or by transfection with p38DN construct, but not control or vector-transfected cell, grew progressively in vivo without entering a state of dormancy (Figure 8D). After 7 d of growth on CAMs the inhibitor treated or the dominant negative p38-expressing cells produced tumors of similar sizes to T-HEp3 cells (see legend to Figure 8). In contrast, inhibition of p38 in AS24 cells caused neither uPAR re-expression nor interruption of dormancy. As in the case of T-HEp3 cells (Figure 8A) and previously published results (Aguirre Ghiso *et al.*, 1999b), pretreatment of the dominant negative p38-expressing D-HEp3 cells or D-HEp3 cells treated with SB203580 with anti-uPAR antibodies reduced the ability of these cells to proliferate in vivo (Figure 8C). Thus, we conclude that uPAR overexpression, through activation of $\alpha5\beta1$-integrin, FN fibrillogenesis, and maintenance of a positive ERK/p38 balance, is responsible for enabling and preserving the tumorigenicity of HEp3 carcinoma cells. In contrast, either blocking of uPAR function or activating p38 ^{MAPK} signaling pathway can force these carcinoma cells into dormancy.

Figure 5. (facing page). cells untreated, or treated with 2 μM SB203580 with or without 30 μM PD98059 (Mek inhibitor) for 36 h, were lysed, and the levels of uPAR protein (top) as well as active (middle) and total (bottom) ERK levels were detected by Western blot. The levels of uPAR and active ERK in T-HEp3 cells served as positive controls. (E) FACS analysis for $\alpha5\beta1$-integrin surface expression using anti-$\alpha5\beta1$-integrin antibodies (clone HA5) in T-HEp3, D-HEp3, or AS24 cells treated with the p38 inhibitor SB203580 (2 μM) for 48 h (SB-D-HEp3 or SB-AS24) or untreated (C-T-HEp3, C-D-HEp3, C-AS24). Isotype-matched IgG was used as control. The numbers indicate the percentages of cells positive for surface $\alpha5\beta1$-integrin. (F) Coimmunoprecipitation of uPAR and $\alpha5\beta1$-integrin in SB203580-treated cells. D-HEp3 cells untreated or treated with 2 μM SB203580 or 2 μM SB203580 and 30 μM PD98059 were lysed, and the cell lysates were subjected to IP with anti-$\alpha5\beta1$-integrin antibodies and the immunoprecipitated proteins were tested by Western blotting with antibodies to $\beta1$-integrin and uPAR.

DISCUSSION

We have identified a new role for uPAR that, through induction of FN fibril formation, influences the state of activation of ERK and p38^{MAPK}. In cells with a high uPAR level (tumorigenic), this receptor associates at high frequency with $\alpha5\beta1$-integrins, inducing their activation. These cells adhere avidly to immobilized FN and show strong activation of the ERK pathway. We now found that, in addition to increased FN adhesion, tumorigenic cells produce FN and assemble it into fibrillar matrix both in culture and when grown on the CAMs of chick embryos. This process is strictly uPAR dependent, because dormant cells with low uPAR, which produce a similar amount of FN, do not form fibrils. Moreover, disruption of the uPAR/integrin complex in tumorigenic cells leads to a drastic reduction in the number of FN fibril-containing cells. Matrix assembly is generally dependent on the state of actin cytoskeleton. Factors such as lysophosphatidic acid by activating GTP-binding protein Rho stimulates actin stress fiber formation, induces fiber contractility, and facilitates matrix assembly (Zhong *et al.*, 1998; Schwarzbauer and Sechler, 1999). HEp3 cells have no stress fibers and have cortically organized actin (Figure 1E) and yet are capable of FN fibril assembly (Figure 1). It is possible that cortical bundles may generate the needed tension or that additional mechanisms for matrix formation exist in different cell and tumor types.

Because we previously determined that just binding of HEp3 cells to immobilized FN is sufficient to induce ERK activation, we wondered what could be the role, if any, of fibrils in maintenance of the tumorigenic phenotype. We found that their presence regulated p38^{MAPK} activation and, indirectly, the level of ERK activity. This conclusion was based on the fact that dormant cells, with no fibrils, had high levels of active p38 and that when fibril formation in T-HEp3 cells was blocked by antibodies or fibrils were disrupted by

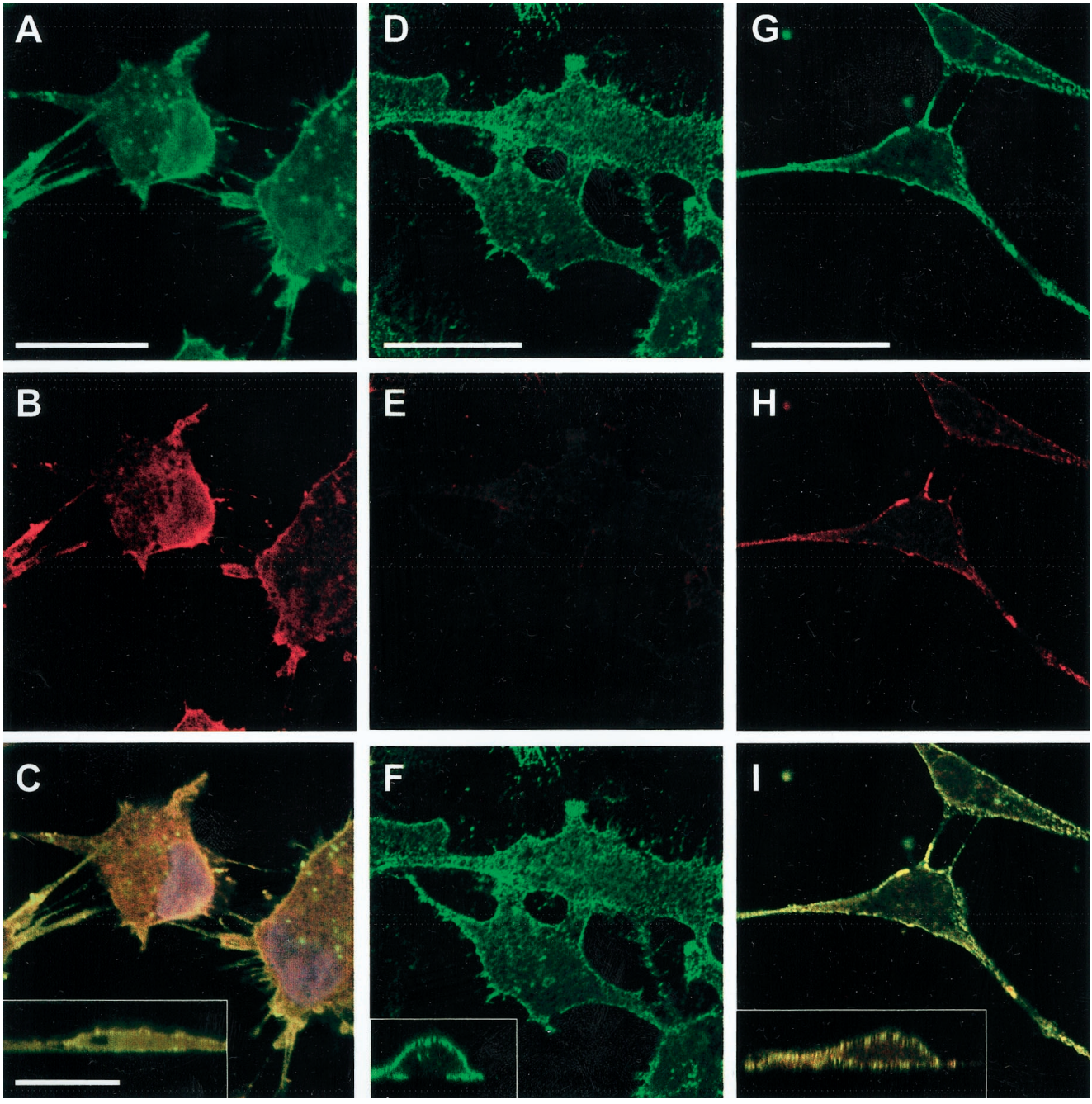

Figure 6. Effect of p38 inhibition on uPAR and β1-integrin surface expression. Untreated T-HEp3 cells (A–C) or D-HEp3 cells treated for 48 h with 2 μM SB203580 (G–I) or DMSO alone (D–F) were fixed and stained, without permeabilization, for β1-integrin (A, D, and G, AIIB2 antibody, green) or uPAR (B, E, H, R2 antibody, red), as described in MATERIALS AND METHODS, and detected by confocal laser scanning IF microscopy. C, F, and I, show the merged image of the uPAR and β1-integrin signals; yellow indicates colocalization of uPAR and β1-integrin signals. A to I are XY sections; insets in C, F, and I are XZ sections of the same cells showing the overlay. Note the high surface (apical and basolateral) expression of uPAR in D-HEp3 cells treated with the p38 inhibitor (compare E with H) that colocalizes with β1-integrin signal (compare F with I and the corresponding insets), which remains unchanged in SB203580-treated cells (compare D and G). Bars, 40 μm.

a III-1C fragment of FN p38 was activated as evidenced by an increase in the phosphorylated form or translocation from the cytoplasm to the nucleus (Figure 3). Although there is evidence that activation of p38 induces its export from the nucleus to the cytoplasm (Ben-Levy *et al.*, 1998), others have shown nuclear translocation upon activation (Cheng and Feldman, 1998). In our cells, activation of p38 causes increased phosphorylation and its translocation to the nucleus.

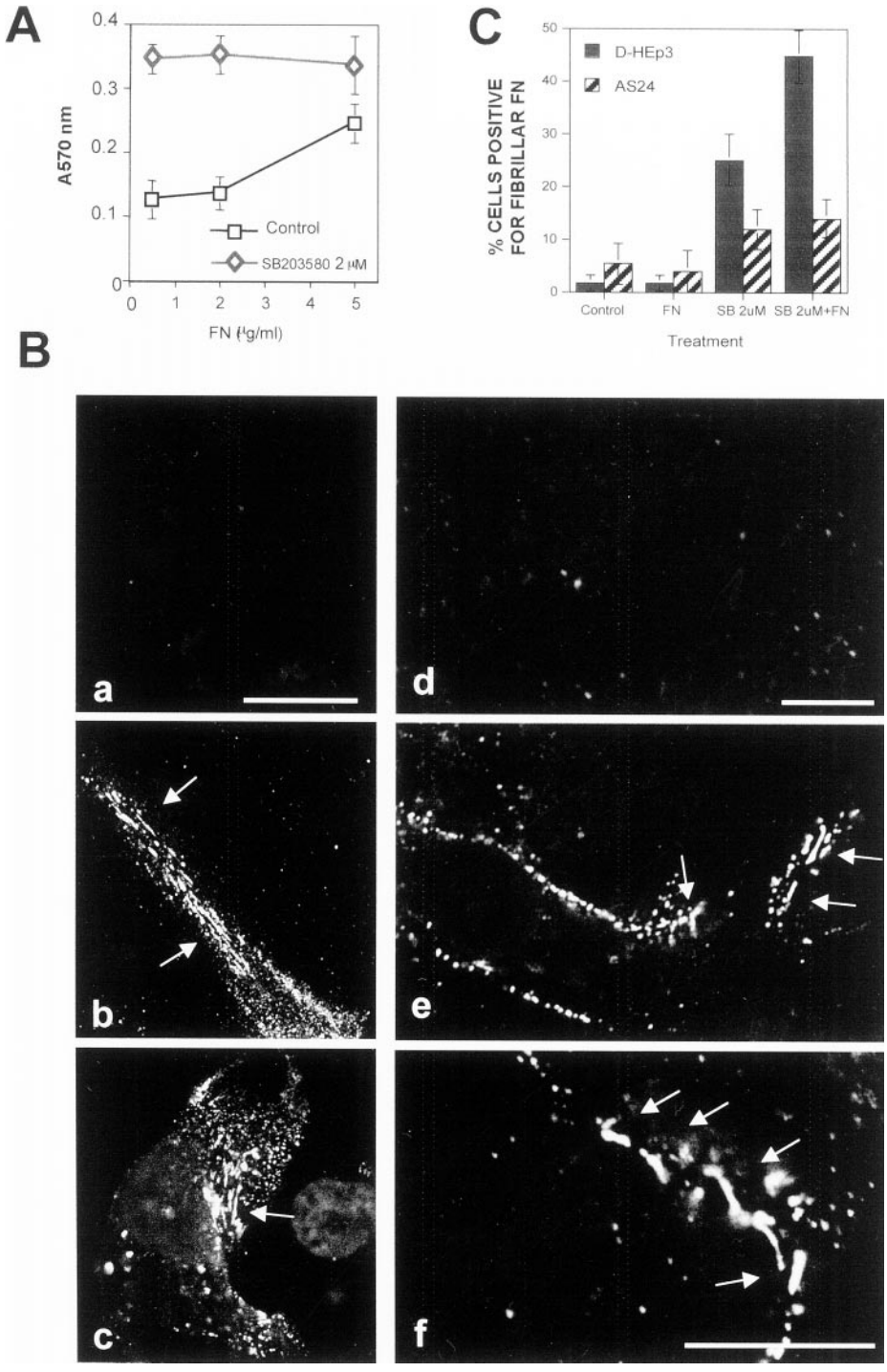

Figure 7. Analysis of the effect of p38 inhibition on $\alpha 5\beta 1$-integrin function. (A) Adhesion of DMSO- or SB203580-treated cells to FN. D-HEp3 cells were treated for 48 h with 0 or 2 μM SB203580 in DMSO, detached, and plated onto FN-coated (0.5–5 μg/ml) wells. After 10 min, the cells were fixed and stained and the attached cells were quantitated as described in MATERIALS AND METHODS. (B) a to c, confocal IF microscopy (a–c, XY sections) for FN fibrils in D-HEp3 cells treated with DMSO alone (a), 2 μM SB203580 (b), or SB203580 with 5 μg/ml human FN (c). Bar, 40 μm. d to f, effect on FN fibril formation of transient transfection of uPAR in D-HEp3. Cells transfected with empty vector (d) or with the vector encoding uPAR (e and f) and grown in serum-containing medium were fixed and stained for FN. Note that only cells transfected with uPAR are able to organize FN into thick bundles and fibrils. A larger magnification of the fibrils is shown in f. Bar, 20 μm. The arrows indicate fibrils. (C) Quantitation of the effect of p38 inhibition on FN fibrillogenesis. Cells (D-HEp3 or AS24) untreated (control) or treated with SB203580 (SB 2 μM) were incubated for 48 h with or without 5 μg/ml FN (FN and SB 2 μM + FN). Cells positive for FN fibrils are shown as percentages of cells with DAPI-positive nuclei.

The finding of p38 activation fit with published observations (Bourdoulous *et al.*, 1998) that showed that in fibroblasts and endothelial cells disruption of FN fibrils induces Cdc42 and $p38^{MAPK}$ activities. The implied role for actin stress fibers in this process, and the fact that HEp3 cells do not have actin stress fibers but rather cortical actin bundles, suggests that the mechanism of FN fibril formation, function and the signaling pathways activated by their presence or their removal, may not be identical in different cell types. However, our preliminary results suggest that Cdc42 is activated when FN fibrils are absent, suggesting that cortical actin may activate similar signaling pathways.

The ability of cancer cells to produce FN and assemble fibrils is unusual because published work indicates mostly

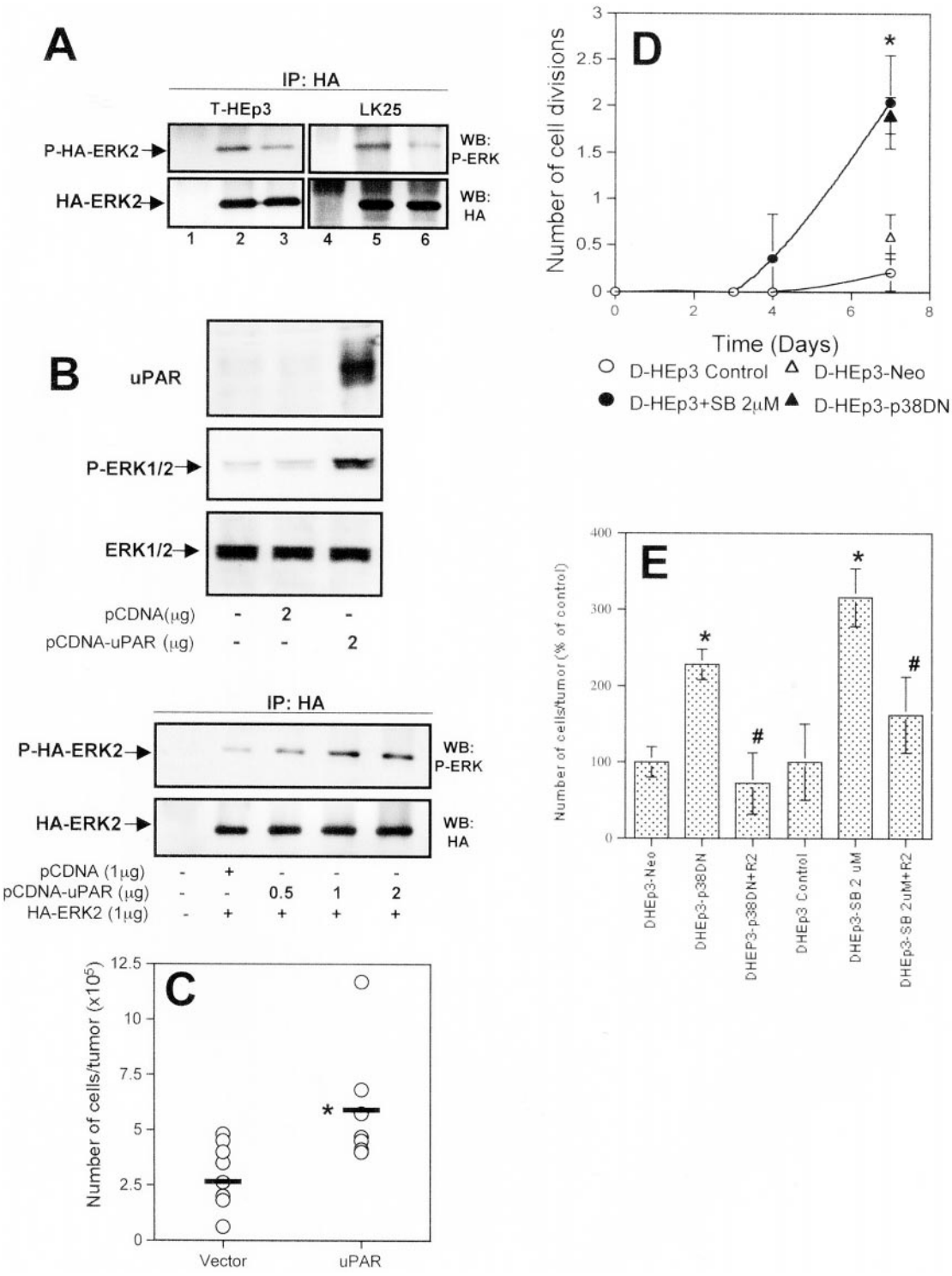

Figure 8. Relevance of uPAR/integrin signaling to ERK and p38 activity in vivo. (A) Down-modulation of ERK activity in vivo by disruption of the uPAR-β1-integrin interaction. T-HEp3 or LK25 cells were transiently transfected with an HA-ERK2 construct (lanes 2, 3, 5, and 6) or mock-transfected (lanes 1 and 4) for 24 h, detached, and incubated in suspension for 30 min with 10 μg/ml R2 and AIIB2 antibodies (lanes 3 and 6) or without antibodies (lanes 2 and 5) and inoculated (2.5×10^6 cells/CAM) onto chick embryo CAMs for an additional 24 h. After in vivo growth, the tumor cell-containing CAM tissue was excised and lysed (see MATERIALS AND METHODS). The lysates were immunoprecipitated with anti-HA antibodies. Total HA-ERK expression (IP: HA, WB: HA) or phosphorylated HA-ERK (IP: HA, WB: P-ERK) was detected by Western blot. (B) Transient expression of uPAR in spontaneous dormant D-HEp3 cells restores high ERK activation. D-HEp3

lower FN levels associated with oncogenic transformation, although these are usually in transformed fibroblasts. Low levels of FN or FN fibrils in transformed cells are presumably due to a lower rate of FN synthesis, a greater level of FN degradation by proteases, and an underexpression of the $\alpha5\beta1$-integrin (Plantefaber and Hynes 1989; Giancotti and Ruoslahti, 1990; Akiyama *et al.*, 1995). Forced expression of FN was shown to inhibit tumorigenicity (Akamatsu *et al.*, 1996). Contrasting with these results, a genetic study showed no role for $\alpha5$ or FN in carcinogenesis (Taverna *et al.*, 1998). Others have argued that it is the state of activation of the integrin that may affect tumor cell growth (Plantefaber and Hynes 1989; Juliano and Varner 1993; Schiller and Bittner, 1995). $\alpha5\beta1$-Integrin, expressed in integrin-deficient colon carcinoma, was shown to be growth suppressive when free of ligand but, when FN bound, was able to induce cell proliferation. Evidence also exists, however, that FN can stimulate growth of melanoma cell lines and primary and metastatic melanomas in a $\alpha5\beta1$-integrin-dependent manner (Mortarini *et al.*, 1992) and that blocking antibodies to $\alpha5\beta1$-integrin inhibits the in vivo growth of human bronchial epithelial tumor cells (Schiller and Bittner, 1995). Also, anchorage-independent growth in soft agar of a murine mammary carcinoma cell line was shown to be dependent on the presence of FN fibrils within the colonies (Saulnier *et al.*, 1996). Such diverse findings do not allow the results from one model to be safely extrapolated to other cells. However, based on our previous work (Aguirre Ghiso *et al.*, 1999b), the current study, and unpublished new data, we conclude that, in tumors that express $\alpha5\beta1$ and high level of uPAR, $\alpha5\beta1$-integrins become activated, they activate the ERK signaling pathway, and by facilitating FN fibrillogenesis, they keep p38 activity suppressed. We are currently testing the generality of this conclusion in other tumor cell types. Conversely, when the high p38 activity found in dormant cells is inhibited by a pharmacological agent (Enslen *et al.*, 1998) or by transfection of a dominant negative form of p38, the negative effect on ERK activity is relieved (Figures 4 and 5), indicating that the two MAPKs (ERK and p38) are functionally linked. Similar results were observed by others (Kusuhara *et al.*, 1998; Singh *et al.*, 1999). We tentatively conclude that the presence of FN fibrils blocks p38 activity while at the same time relieving the inhibitory effect (direct or indirect) of p38 on ERK. This allows for the flow of a mitogenic signal from the uPA/uPAR/$\alpha5\beta1$/FN complex, which is sufficiently potent to exceed a threshold of ERK activity required for in vivo growth. Conversely, when the p38 pathway is activated, as in low uPAR-expressing cells, not only the mitogenic signal from ERK is reduced but cell cycle arrest, due to inhibition of cycline D1 expression (Lavoie *et al.*, 1996; Ellinger-Ziegelbauer *et al.*, 1999) or to the effect on the mitotic spindle assembly checkpoint (Takenaka *et al.*, 1998), may be activated. In support of this conclusion, activation of p38 has been shown to be responsible for induction of growth arrest in prostate cancer metastasis (Teng *et al.*, 1997) and for reversion of Ras-induced transformation (Ellinger-Ziegelbauer *et al.*, 1999)

An important finding that further implicates uPAR in fibrillogenesis and control of the balance between the two MAPK pathways is the finding that inhibition of p38 activity in dormant cells produces a biphasic wave of ERK activation, first induced within minutes generated by an as yet unknown mechanism, and a second wave, strong and persisting for days (Figure 5, A–C). As previously shown (Lengyel *et al.*, 1997; Aguirre Ghiso *et al.*, 1999a) the first wave of ERK activation causes an increase in uPAR-mRNA and protein (Figure 5). The observed increase in the uPAR-mRNA level may represent the net sum of transcriptional activation by ERK and decreased mRNA stability due to inhibition of p38 (Montero and Nagamine, 1999). The newly synthesized uPAR coimmunoprecipitates with (Figure 5F) and colocalizes with the surface $\beta1$-integrin (Figure 6), initiating a positive feedback loop that converts the low ERK/p38 ratio of dormant cells to the high ratio existing in tumorigenic cells. This is reflected in restoration of their ability to adhere more efficiently to immobilized FN, to organize FN into fibrils, and to form tumors on CAMs (Figures 7 and 8). The restoration of the in vivo growth of the p38-inhibited D-HEp3 cells was reversed by pretreatment of these cells with an anti-uPAR (R2) antibody (Figure 8E). The inhibition of in vivo growth by R2 antibodies is similar to that we described for T-HEp3 cells (Aguirre Ghiso *et al.*, 1999b), indicating that, whether endogenously expressed or induced by inhibition of p38, uPAR and its interaction with the $\alpha5\beta1$-integrin have a regulatory function in tumorigen-

Figure 8 (facing page). cells were transiently transfected with 2 μg of uPAR-cDNA or control plasmids and uPAR expression or ERK activation were examined by Western blot of whole cell lysates (top three panels). In the bottom two panels D-HEp3 cells were transiently cotransfected with empty vector or HA-ERK2 (1 μg) constructs or with increasing amounts (0.5–2 μg) of uPAR cDNA plasmid. HA-ERK was immunoprecipitated with anti-HA and blotted with anti-phospho-ERK or with anti-HA antibodies. Note that uPAR expression generates a strong activation of ERK. (C) Effect of transient expression of uPAR on the growth of D-HEp3 cells in vivo. D-HEp3 cells transfected with empty vector or with the uPAR-encoding vector were grown for 48 h and after detachment the cells were inoculated onto 9-d-old CAMs. The number of cells per tumor was determined as described in MATERIALS AND METHODS. The horizontal lines indicate the mean. $^*P < 0.02$ as determined by Mann-Whitney test. (D) Effect of p38 inhibition on in vivo growth of dormant cells. D-HEp3 cells pretreated with 2 μM SB203580 or left untreated for 48 h or D-HEp3-neo and D-HEp3-p38DN cells were detached and inoculated at 4×10^5 cells per 9-d-old chick embryo CAM. After 3, 4, and 7 d the number of tumor cells in the tumor nodules was quantitated as described in MATERIALS AND METHODS. The graph shows the mean number and SE of the population cell divisions. Note that only D-HEp3 cells treated with SB203580 or D-HEp3-p38DN cells developed growing tumors. Their growth rate was similar to that of T-HEp3 cells, which divided ~3.2 times in 7 d and were not affected by SB203580 treatment (approximately three divisions); $^*P < 0.001$ Mann-Whitney test. Unlike D-HEp3 cells, AS24 cells were unable to form growing tumors even after treatment with 2–4 μM SB203580 for 48 h. (E) Effect of anti-uPAR antibodies on the growth of D-HEp3 cells in which p38 activity was inhibited. D-HEp3-p38DN or D-HEp3 cells pretreated with 2 μM SB203580 for 48 h were incubated in suspension with 10 μg/ml anti-uPAR antibody (R2) or left untreated. The cells were then inoculated onto 9- to 10-d-old chick embryo CAMs and after 4 d the number of cell per tumor nodules was determined. These groups were compared with the growth of parental, untreated D-HEp3 or D-HEp3-neo cells. The results are expressed as percentages of control (mean and SD). $^*P < 0.01$, D-HEp3- p38DN or D-HEp3-SB2 μM versus D-HEp3-neo or -control cells. # $P < 0.01$, R2 antibody treated versus untreated D-HEp3-p38DN or D-HEp3-SB2 μM cells as determined by Mann-Whitney test.

esis and dormancy. To further ensure that uPAR is responsible for the restoration of tumorigenicity in p38-inhibited D-HEp3, the direct effect of uPAR re-expression was examined by transfecting the D-HEp3 cells with a uPAR-encoding construct. The high level of uPAR that was detected in these cells (Figure 8B) was sufficient to activate ERK (Figure 8B) to re-establish FN fibrillogenesis (Figure 7B) and to rescue these cells from dormancy (Figure 8C).

It is also of interest to note that in AS24 cells the inhibition of p38 induces and maintains only the first wave of ERK activation (Figure 4C), without a subsequent uPAR induction, presumably because the newly transcribed uPAR-mRNA is inhibited by the uPAR-antisense. In these cells there is no escape from dormancy in vivo, implicating again uPAR as an important regulator of tumorigenicity.

Our results can be assembled into the following working model: in tumorigenic (uPAR-rich) HEp3 cells in which uPA/bound uPAR is highly overexpressed, the frequency of interactions between uPAR and $\alpha5\beta1$-integrin is high. These interactions keep a large proportion of the integrin in a high-affinity/avidity state, which enables their efficient binding to FN and activation of ERK. In addition, the high-affinity/avidity states of integrins mediate FN fibril formation, which through a signal involving integrins, cytoskeleton and, most likely, a small G-protein suppress p38 activity. The combination of robust ERK activity and p38 inhibition generates a mitogenic signal that is potent enough to promote tumorigenicity. Moreover, activation of ERK signaling sustains a positive feedback loop by promoting uPA and uPAR transcription and fibril formation. When uPAR is down-regulated, $\alpha5\beta1$-integrins shift to a low-affinity/avidity state, which is not sufficient to generate a strong ERK activation and FN fibril formation. The lack or disruption of the FN matrix changes the structural signals the cells receive, leading to activation of the p38 pathway, probably through activation of Cdc42. Activated p38 inhibits ERK activity, creating an inverse balance between these two antagonizing pathways and causing tumor dormancy.

We presume that under in vivo conditions a continuous competition exists between fibril formation and FN degradation by tumor proteases but that once fibrils are formed they become partially resistant to proteolytic degradation. Our results (Figure 1C) showing FN fibril formation in T-HEp3 tumors in vivo support this conclusion. Because tumor cell attachment to the matrix and its degradation are important in proliferation and invasive movement of cancer cells, it is likely that in vivo matrix assembly and proteolysis exist in a state of a dynamic balance. There is also evidence that both uPAR level and its biochemical structure and functions are continuously modulated in vivo. For example, it is known that domain 1 of uPAR is highly susceptible to cleavage by several proteases (Montuori *et al.*, 1999) and that the truncated receptor does not bind uPA and may not be able to interact with integrins (Montuori *et al.*, 1999), creating conditions that may curtail the magnitude of ERK activation. Disseminating cells with cleaved surface-uPAR would have a reduced chance to establish a proliferative interaction with the matrix of the target organ and would enter dormancy. The insight into tumor dormancy induction gained through our work may provide new avenues for therapy.

ACKNOWLEDGMENTS

We are deeply grateful to Dr. Sandy Masur and members of her laboratory in the Department of Ophthalmology and Dr. Scott Henderson, Director of Fluorescence and Confocal Microscopy Shared Facility, for their invaluable help with the immunocytochemistry studies. Confocal laser scanning microscopy was supported with funding from a National Science Foundation Major Research Instrumentation grant (DBI-9724504) of the Mount Sinai School of Medicine Microscopy Center. We would like to thank rotating Ph.D. students Mr. Dana Lukin and Ms. Felicia Stein and a visiting Ph.D. student from The University of Quilmes, Argentina, Lic. Hernán Farina for help with some of the experiments. We thank Dr. Rafael Mira y Lopez for critical reading of the manuscript. The continuous encouragement and support of Dr. Samuel Waxman is gratefully acknowledged. We also thank Dr. Iñigo Santamaria Ruiz de Azua (Mount Sinai School of Medicine) for the uPAR-expressing plasmid, Dr. Fillipo Giancotti (Memorial Sloan Kettering Cancer Center, New York) for the HA-ERK2 construct, Dr. Michael Ploug (Finsen Laboratory, Copenhagen, Denmark) for the gift of R2 antibodies, Dr. Steve Rosenberg (Chiron Corp) for peptide 25, Dr. Errki Ruoslahti for the gift of the III11-C FN fragment, and Dr. Caroline Damsky (University of California, San Francisco) for AIIB2 and BIIG2 antibodies. This work was supported by U.S. Public Health Service Research grant (CA-40758 to L.O.), National Institutes of Health/Mt. Sinai School of Medicine Medical Scientist Training Program (to D.L), and The Samuel Waxman Cancer Research Foundation.

REFERENCES

Aguirre Ghiso, J.A., Alonso, D.F., Farias, E.F., Gomez, D.E., and de Kier Joffe, E.B. (1999a). Deregulation of the signaling pathways controlling urokinase production: its relationship with the invasive phenotype. Eur. J. Biochem. *263*, 295–304.

Aguirre Ghiso, J.A., Kovalski, K., and Ossowski, L. (1999b). Tumor dormancy induced by downregulation of urokinase receptor in human carcinoma involves integrin and MAPK signaling. J. Cell Biol.*147*, 89–104.

Akamatsu, H., Ichihara-Tanaka, K., Ozono, K., Kamiike, W., Matsuda, H., and Sekiguchi, K. (1996). Suppression of transformed phenotypes of human fibrosarcoma cells by overexpression of recombinant fibronectin. Cancer. Res. *56*, 4541–4546.

Akiyama, S.K., Olden, K., and Yamada, K.M. (1995). Fibronectin and integrins in invasion and metastasis. Cancer Metastasis Rev. *14*, 173–189.

Ben-Levy, R., Hooper, S., Wilson, R., Paterson, H.F., and Marshall, C.J. (1998). Nuclear export of the stress-activated protein kinase p38 mediated by its substrate MAPKAP kinase-2. Curr. Biol. *8*, 1049–1057.

Bourdoulous, S., Orend, G., MacKenna, D.A., Pasqualini, R., and Ruoslahti, E. (1998). Fibronectin matrix regulates activation of RHO and CDC42 GTPases and cell cycle progression. J. Cell Biol.*143*, 267–276.

Chandler, L.A., Ehretsmann, C.P., and Bourgeois, S. (1994). A novel mechanism of Ha-ras oncogene action: regulation of fibronectin mRNA levels by a nuclear posttranscriptional event. Mol. Cell. Biol.*14*, 3085–3093.

Cheng, H-L., and Feldman, E.L. (1998). Bidirectional regulation of p38 kinase and c-Jun N-terminal protein kinase by insulin-like growth factor-I. J. Biol. Chem. *273*, 14560–14565.

Ellinger-Ziegelbauer, H., Kelly, K., and Siebenlist, U. (1999). Cell cycle arrest and reversion of Ras-induced transformation by a conditionally activated form of mitogen-activated protein kinase kinase kinase 3. Mol. Cell. Biol.*19*, 3857–3868.

Enslen, H., Raingeaud, J., and Davis, R.J. (1998). Selective activation of p38 mitogen-activated protein (MAP) kinase isoforms by the MAP kinase kinases MKK3 and MKK6. J. Biol. Chem. *273*, 1741–1748.

Eyers, P.A., Craxton, M., Morrice, N., Cohen, P., and Goedert, M. (1998). Conversion of SB 203580-insensitive MAP kinase family members to drug-sensitive forms by a single amino-acid substitution. Chem. Biol. *5*, 321–328.

Giancotti, F.G., and Ruoslahti, E. (1990). Elevated levels of the alpha 5 beta 1 fibronectin receptor suppress the transformed phenotype of Chinese hamster ovary cells. Cell *60*, 849–859.

Gu, H., and Oliver, N. (1995). Transcriptional repression of fibronectin gene expression in v-src transformation. Exp. Cell Res. *217*, 428–439.

Juliano, R.L., and Varner, J.A. (1993). Adhesion molecules in cancer: the role of integrins. Curr. Opin. Cell Biol. *5*, 812–818.

Kusuhara, M., Takahashi, E., Peterson, T.E., Abe, J., Ishida, M., Han, J., Ulevitch, R., and Berk, B.C. (1998). p38 kinase is a negative regulator of angiotensin II signal transduction in vascular smooth muscle cells: effects on Na+/H+ exchange and ERK1/2. Circ. Res. *83*, 824–831.

Lavoie, J.N., L'Allemain, G., Brunet, A., Muller, R., and Pouyssegur, J. (1996). Cyclin D1 expression is regulated positively by the p42/p44MAPK and negatively by the p38/HOGMAPK pathway. J. Biol. Chem. *271*, 20608–20616.

Lengyel, E., Wang, H., Gum, R., Simon, C., Wang, Y., and Boyd, D. (1997). Elevated urokinase-type plasminogen activator receptor expression in a colon cancer cell line is due to a constitutively activated extracellular signal-regulated kinase-1-dependent signaling cascade. Oncogene *14*, 2563–2573.

Mayor, S., Rothberg, K.G., and Maxfield, F.R. (1994). Sequestration of GPI-anchored proteins in caveolae triggered by cross-linking. Science *264*, 1948–1951.

Molnar, A., Theodoras, A.M., Zon, L.I., and Kyriakis, J.M. (1997). Cdc42Hs, but not Rac1, inhibits serum-stimulated cell cycle progression at G1/S through a mechanism requiring p38/RK. J. Biol. Chem. *272*, 13229–13235.

Montero, L., and Nagamine, Y. (1999). Regulation by p38 mitogen activated protein kinase- and uridylate-rich element-mediated urokinase-type plasminogen activator (uPA) messenger RNA stability and uPA-dependent in vitro cell invasion. Cancer. Res. *59*, 5286–5293.

Montuori, N., Rossi, G., and Ragno, P. (1999). Cleavage of urokinase receptor regulates its interaction with integrins in thyroid cells. FEBS Lett. *460*, 32–36.

Mortarini, R., Gismondi, A., Santoni, A., Parmiani, G., and Anichini, A. (1992). Role of the alpha 5 beta 1 integrin receptor in the proliferative response of quiescent human melanoma cells to fibronectin. Cancer. Res. *52*, 4499–4506.

Ossowski, L., and Reich, E. (1983). Changes in malignant phenotype of a human carcinoma conditioned by growth environment. Cell *33*, 323–333.

Plantefaber, L.C., and Hynes, R.O. (1989). Changes in integrin receptors on oncogenically transformed cells. Cell *56*, 281–290.

Raingeaud, J., Gupta, S., Rogers, J.S., Dickens, M., Han, J., Ulevitch, R.J., and Davis, R.J. (1995). Pro-inflammatory cytokines and environmental stress cause p38 mitogen-activated protein kinase activation by dual phosphorylation on tyrosine and threonine. J. Biol. Chem. *270*, 7420–7426.

Saulnier, R., Bhardwaj, B., Klassen, J., Leopold, D., Rahimi, N., Tremblay, E., Mosher, D., and Elliott, B. (1996). Fibronectin fibrils and growth factors stimulate anchorage-independent growth of a murine mammary carcinoma. Exp. Cell Res. *222*, 360–369.

Schiller, J.H., and Bittner, G. (1995). Loss of the tumorigenic phenotype with in vitro, but not in vivo, passaging of a novel series of human bronchial epithelial cell lines: possible role of an alpha 5/beta 1-integrin-fibronectin interaction. Cancer. Res. *55*, 6215–6221.

Schwarzbauer, J.E., and Sechler, J.L. (1999). Fibronectin fibrillogenesis: a paradigm for extracellular matrix assembly. Curr. Opin. Cell Biol. *11*, 622–627.

Singh, R.P., Dhawan, P., Golden, C., Kapoor, G.S., and Mehta, K.D. (1999). One-way cross-talk between p38MAPK and p42/44MAPK inhibition of p38MAPK induces low density lipoprotein receptor expression through activation of the p42/44 MAPK casacade. J. Biol. Chem. *274*, 19593–19600.

Takenaka, K., Moriguchi, T., and Nishida, E. (1998). Activation of the protein kinase p38 in the spindle assembly checkpoint and mitotic arrest. Science *280*, 599–602.

Taverna, D., Ullman-Cullere, M., Rayburn, H., Bronson, R.T., and Hynes, R.O. (1998). A test of the role of alpha5 integrin/fibronectin interactions in tumorigenesis. Cancer. Res. *58*, 848–853.

Teng, D.H., Perry, W. L., 3rd, Hogan, J. K., Baumgard, M., Bell, R., Berry, S., Davis, T., Frank, D., Frye, C., Hattier, T., Hu, R., Jammulapati, S., Janecki, T., Leavitt, A., Mitchell, J.T., Pero, R., Sexton, D., Schroeder, M., Su, P.H., Swedlund, B., Kyriakis, J.M., Avruch, J., Bartel, P., Wong, A.K., Tavtigian, S.V., et al. (1997). Human mitogen-activated protein kinase kinase 4 as a candidate tumor suppressor. Cancer Res. *57*, 4177–4182.

Toolan, H.W. (1954). Transplantable human neoplasms maintained in cortisone-treated laboratory animals: HS#1,H.Ep#1, H.Ep.#2, H.Ep.#3, and H.Emb.#1. Cancer Res. *14*, 660–666.

Wei, Y., Lukashev, M., Simon, D.I., Bodary, S.C., Rosenberg, S., Doyle, M.V., and Chapman, H.A. (1996). Regulation of integrin function by the urokinase receptor. Science *273*, 1551–1555.

Werb, Z., Tremble, P.M., Behrendtsen, O., Crowley, E., and Damsky, C.H. (1989). Signal transduction through the fibronectin receptor induces collagenase and stromelysin gene expression. J. Cell Biol. *109*, 877–889.

Werbajh, S.E., Urtreger, A.J., Puricelli, L.I., de Lustig, E.S., Bal de Kier Joffe, E., and Kornblihtt, A.R. (1998). Downregulation of fibronectin transcription in highly metastatic adenocarcinoma cells. FEBS Lett. *440*, 277–281.

Wu, C., Keivens, V.M., O'Toole, T.E., McDonald, J.A., and Ginsberg, M.H. (1995). Integrin activation and cytoskeletal interaction are essential for the assembly of a fibronectin matrix. Cell *83*, 715–724.

Xia, Z., Dickens, M., Raingeaud, J., Davis, R.J., and Greenberg, M.E. (1995). Opposing effects of ERK and JNK-p38 MAP kinases on apoptosis. Science *270*, 1326–1331.

Yu, W., Kim, J., and Ossowski, L. (1997). Reduction in surface urokinase receptor forces malignant cells into a protracted state of dormancy. J. Cell Biol.*137*, 767–777.

Zhong, C., Chrzanowska-Wodnicka, M., Brown, J., Shaub, A., Belkin, A.M., and Burridge, K. (1998). Rho-mediated contractility exposes a cryptic site in fibronectin and induces fibronectin matrix assembly. J. Cell Biol. *141*, 539–551.